An Evolutionarily Conserved DOF-CONSTANS Module Controls Plant Photoperiodic Signaling[1][OPEN]

Eva Lucas-Reina, Francisco J. Romero-Campero, José M. Romero, and Federico Valverde*

Institute for Plant Biochemistry and Photosynthesis, Plant Development Unit, Consejo Superior de Investigaciones Científicas and Universidad de Sevilla, 41092 Seville, Spain (E.L.-R., J.M.R., F.V.); and Departamento de Ciencias de la Computación e Inteligencia Artificial, Grupo de Investigación en Computación Natural, Universidad de Sevilla, 41012 Seville, Spain (F.J.R.-C.)

ORCID IDs: 0000-0002-4113-2064 (E.L.-R.); 0000-0001-9834-030X (F.J.R.-C.); 0000-0002-4621-5934 (J.M.R.); 0000-0001-8063-0974 (F.V.).

The response to daylength is a crucial process that evolved very early in plant evolution, entitling the early green eukaryote to predict seasonal variability and attune its physiological responses to the environment. The photoperiod responses evolved into the complex signaling pathways that govern the angiosperm floral transition today. The *Chlamydomonas reinhardtii DNA-Binding with One Finger* (*CrDOF*) gene controls transcription in a photoperiod-dependent manner, and its misexpression influences algal growth and viability. In short days, *CrDOF* enhances *CrCO* expression, a homolog of plant *CONSTANS* (*CO*), by direct binding to its promoter, while it reduces the expression of cell division genes in long days independently of CrCO. In Arabidopsis (*Arabidopsis thaliana*), transgenic plants overexpressing *CrDOF* show floral delay and reduced expression of the photoperiodic genes *CO* and *FLOWERING LOCUS T*. The conservation of the *DOF-CO* module during plant evolution could be an important clue to understanding diversification by the inheritance of conserved gene toolkits in key developmental programs.

Due to their sessile lifestyle, vascular plants have evolved intricate genetic regulatory pathways to control essential developmental processes in response to changes in the environment. One of the most distinctive processes is the floral transition (Amasino, 2010), which integrates information from endogenous and external signals to guarantee reproductive success (Valverde, 2011). In Arabidopsis (*Arabidopsis thaliana*), the *CONSTANS* (*CO*) gene plays a central role in the control of photoperiodic flowering by triggering the expression of *FLOWERING LOCUS T* (*FT*) in the leaf vascular tissue (An et al., 2004). *FT* codes for a major component of the florigenic signal that moves through the phloem to induce flower differentiation at the shoot apex (Corbesier et al., 2007; Tamaki et al., 2007). *CO* and *FT* are controlled at the transcriptional level by a circadian and photoperiodic signal through the *FLAVIN-BINDING*, *KELCH REPEAT*, *F-BOX1* (*FKF1*), *GIGANTEA* (*GI*), and *CYCLING DOF FACTOR* (*CDF*) genes (Song et al., 2012). In long days (LD), blue light induces the assembly of the FKF1-GI complex that promotes the proteasome-mediated degradation of the CDFs, a four-member family of DNA-binding with One Finger (DOF) transcription factors (TFs) that bind to *CO* and *FT* promoters, repressing their expression (Song et al., 2012). The photoperiodic pathway is probably the most conserved of the flowering signaling responses in spermatophytes (Amasino, 2010) and can be traced back to chlorophytes, where *CrCO*, a *CO* homologous gene from *Chlamydomonas reinhardtii*, was identified (Serrano et al., 2009). *CrCO* is involved in the regulation of starch synthesis and cell growth in the alga (Serrano et al., 2009), two processes that are also regulated by the *CONSTANS-LIKE* (*COL*) gene family members in vascular plants (Valverde, 2011; Romero-Campero et al., 2013). In addition, transgenic plants overexpressing *CrCO* under the control of a constitutive or phloem-specific promoter flowered earlier than wild-type plants and complemented *co* mutants (Serrano et al., 2009).

CDFs constitute a subgroup of DOF TFs (Imaizumi et al., 2005; Fornara et al., 2009), characterized by the presence of a 52-amino acid DOF domain, a single zinc finger that binds to the DNA consensus sequence AAAG. DOFs can work as transcriptional activators or inhibitors, depending on the protein and the target gene concerned (Noguero et al., 2013). The DOF domain is bifunctional, as it can participate in DNA-binding and protein-protein interactions (Yanagisawa, 1997). DOFs have been described exclusively in plants and are involved in numerous processes, from tissue differentiation to metabolic regulation and seed development.

[1] This work was supported by Ministerio de Economía y Competitividad (project nos. BIO2011–28847–C02–00 and BIO2014–52425–P and Juan de la Cierva program funding to F.J.R.-C.), by the Junta de Andalucía (grant no. P08–AGR–03582), by the European Regional Development Fund, and by the Consejo Superior de Investigaciones Científicas-Junta de Ampliación de Estudios and the European Union European Social Fund (fellowship to E.L.-R.).

* Address correspondence to federico.valverde@ibvf.csic.es.

The author responsible for distribution of materials integral to the findings presented in this article in accordance with the policy described in the Instructions for Authors (www.plantphysiol.org) is: Federico Valverde (federico.valverde@ibvf.csic.es).

J.M.R. and F.V. participated in the design of the experiments; E.L.-R. performed most of the experiments; E.L.-R., F.J.R.-C., J.M.R., and F.V. performed the bioinformatic analyses; E.L.-R., F.J.R.-C., J.M.R., and F.V. collaborated in the writing of the article.

[OPEN] Articles can be viewed without a subscription.

www.plantphysiol.org/cgi/doi/10.1104/pp.15.00321

They are widely distributed, with numerous genomic copies, in both gymnosperms and angiosperms and constitute a small gene family in some bryophytes such as the moss *Physcomitrella patens*. A single-copy *CrDOF* gene from *C. reinhardtii* (Moreno-Risueno et al., 2007; Shigyo et al., 2007) represents the ancestor of the DOF TF family. DOFs are absent in heterotrophic eukaryotes, red algae, and heterokonts (Hernando-Amado et al., 2012), so modern DOFs, similar to COLs, constitute a family of TFs exclusive of the green lineage (Serrano et al., 2009).

Here, we show that *CrDOF* induces *CrCO* expression in short days (SD) and is a general repressor of algal gene expression in LD. *CrDOF* expression in Arabidopsis reproduces CDF function by reducing *CO* and *FT* transcript levels and delaying flowering. The *DOF-CO* evolutionarily conserved signaling module constitutes a direct clue to how developmental responses may have evolved from unicellular algae to multicellular plants by the parallel evolution of developmental gene toolkits.

RESULTS

C. reinhardtii CrDOF Defines a Subfamily of DOF TFs Closely Related to CDFs in Arabidopsis

In version 5.5 of the *C. reinhardtii* genome annotation (http://phytozome.jgi.doe.gov/pz/portal.html), a single-copy gene (Cre12.g521150) at positions 4,424,576 to 4,431,469 on chromosome 12 (*CrDOF*) showed a significant identity with DOF TFs (Moreno-Risueno et al., 2007). In order to characterize its gene structure, three complementary DNA (cDNA) clones from the Kazusa open reading frame (ORF) collection (http://www.kazusa.or.jp) were sequenced. The *CrDOF* coding sequence was 1,875 bp long and was identical to the draft genome sequence (Merchant et al., 2007) at the 3′ end but shorter at the 5′ end (Fig. 1A). This was further confirmed by the alignment of the RNA sequencing (RNAseq) data to the predicted gene structure (Fig. 1B).

Using the CrDOF amino acid sequence, a BLAST search in several representative plant species was run and 84 different putative DOF proteins identified (Supplemental Table S1). These sequences were used to construct a phylogenetic tree (Fig. 1C) using the MEGA5 program (Tamura et al., 2011). This phylogenetic tree presents four clusters, including chlorophyte (cluster 1), bryophyte (cluster 2), and spermatophyte (clusters 3a and cluster 3b-3c) sequences. Cluster 3b-3c enclosed the Arabidopsis photoperiodic CDFs (Imaizumi et al., 2005; Fornara et al., 2009), closely aligned with chlorophyte sequences including CrDOF. This protein family also comprised other DOFs from *Populus*, *Zea*, and *Oryza* spp. that may represent putative photoperiodic DOF TFs, such as OsDOF12, which has been

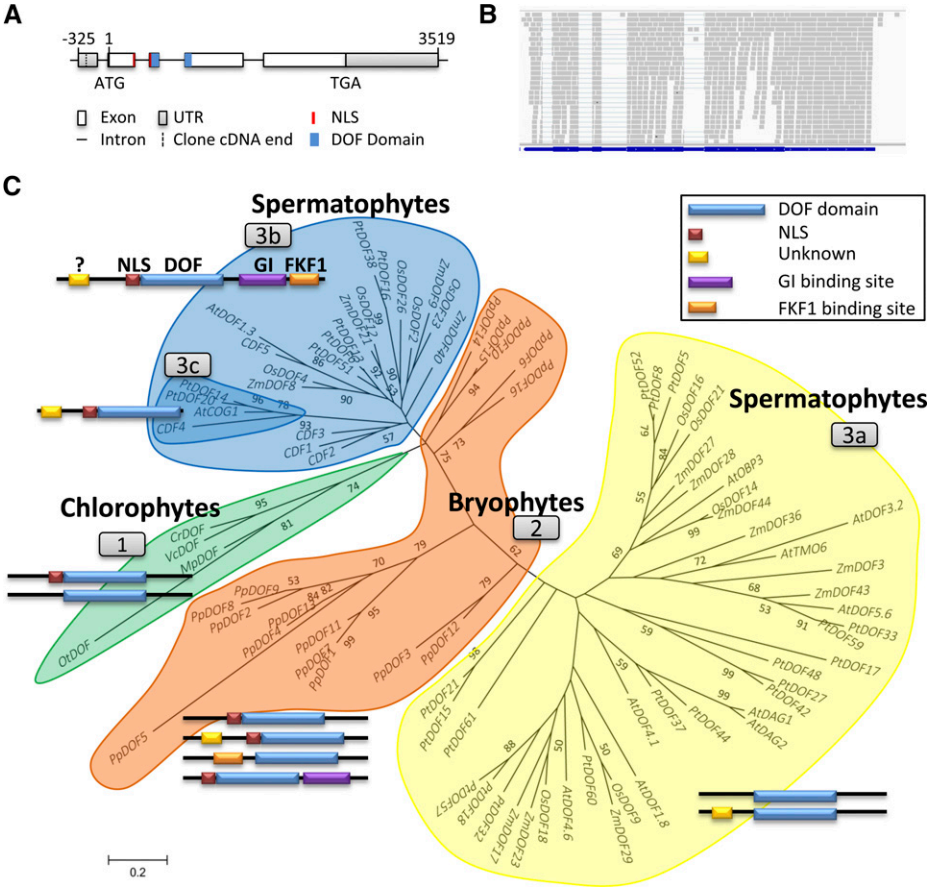

Figure 1. Phylogenetic tree and domain evolution of DOF proteins. A, *CrDOF* gene structure. Squares represent exons, and lines represent introns. The DOF domain is in blue and the nuclear localization signal (NLS) is in red. B, Alignment of sequences obtained from RNAseq (gray) with the *CrDOF* gene structure (blue). C, Evolutionary relationship of 84 DOF proteins from eight species of the Viridiplantae linage. Three clusters pertaining to evolutionary grade are shown: chlorophytes (group 1), bryophytes (group 2), and spermatophytes (groups 3a–3c). Neighbor joining with the substitution model JTT + G 0.54 was the algorithm employed. The bootstrap number was 500. For abbreviations and protein accession numbers, see Supplemental Table S1. The domain structures of DOF proteins from each cluster are depicted beside each group. DOF domains are shown in blue, NLS in red, an unknown domain in yellow, and GI- and FKF1-binding sites in purple and orange, respectively. Only domains with a significant score in the MEME program are shown.

shown to be involved in photoperiodic flowering in rice (*Oryza sativa*; Li et al., 2009). No *Physcomitrella* spp. protein was included in this cluster; rather, they formed a group on their own, bridging chlorophyte with spermatophyte sequences. Subfamily 3a included DOF proteins from Arabidopsis, poplar (*Populus* spp.), maize (*Zea mays*), and rice that have been shown to be involved in diverse processes other than photoperiodic flowering, such as DOF AFFECTING GERMINATION1,2 (AtDAG1,2), involved in germination in Arabidopsis (Papi et al., 2000; Gualberti et al., 2002), or ZmDOF3 (PROLAMIN-BOX BINDING FACTOR1), involved in storage protein synthesis in maize seeds (Vicente-Carbajosa et al., 1997).

CDF proteins have a characteristic domain structure (Fig. 1C, group 3b) with a conserved DOF domain (blue) preceded by an NLS (red). C-terminal domains for GI-binding (purple) and FKF1-binding (orange) sites are specific for CDFs, as they participate in the interactions that control their posttranslational regulation (Kloosterman et al., 2013). A conserved N-terminal domain of unknown function (yellow) is also present. The ancestral algal DOF protein from group 1 (Fig. 1C) contains the conserved DOF domain and the NLS signal but lacks any other clear domain. In *P. patens*, although GI and FKF1 proteins have not been identified in its genome (Rensing et al., 2008), different DOF proteins (cluster 2) include regions that resemble the GI- and FKF1-binding sites that together with the yellow domains later evolved into the modern plant DOF domains in CDFs (clusters 3b and 3c) and other DOFs (cluster 3a; Kloosterman et al., 2013). Therefore, the original algal DOF TF acquired new domains that defined their regulation and function (Fig. 1C), as suggested by the close association between domain structure and function observed in the phylogenetic tree.

CrDOF Is Differentially Expressed under Diverse Photoperiod Conditions in *C. reinhardtii*

Arabidopsis *CDFs* are differentially expressed under diverse daylengths in order to correctly time the expression of *CO* and confer a photoperiodic response to flowering (Imaizumi et al., 2005). *CrDOF* expression in *C. reinhardtii* was monitored under LD and SD every 4 h for 24 h starting at Zeitgeber time 0 (ZT0), the moment the lights are switched on. *CrDOF* mRNA levels were higher in LD than in SD, and the expression profile resembled that of *CDFs* in Arabidopsis: a peak of expression in the late night and early morning (Fornara et al., 2009; Fig. 2A). When the expression was monitored during a 24-h LD followed by 48 h in continuous light (LL) or continuous dark (DD), the expression of *CrDOF* continued oscillating (Fig. 2B). This was particularly true for LL, but even a slight oscillation in DD was observed after 48 h, indicating a circadian influence.

To monitor the presence of CrDOF protein, we produced polyclonal antibodies by immunizing rabbits with a recombinant CrDOF purified from *Escherichia coli* (see "Materials and Methods"). These antibodies were used to detect CrDOF in extracts from the recombinant bacteria and from *C. reinhardtii* (Fig. 2C). While the recombinant protein showed a molecular mass (MM) of 60 kD, which is close to its predicted size (62 kD), the extract from *C. reinhardtii* showed a unique band of approximately 100 kD. Because we used SDS-PAGE conditions, the result suggested that the 100-kD band

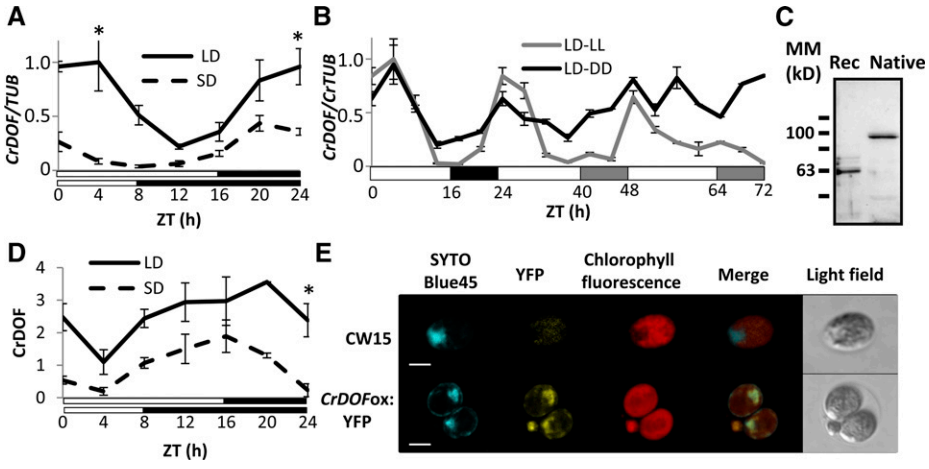

Figure 2. *CrDOF* expression is influenced by daylength and the circadian clock. A, *CrDOF* transcript levels in CW15 during a 24-h course in LD (solid line) and SD (dashed line). Data are from three independent experiments ± SE. B, Circadian expression of *CrDOF* in a 24-h LD followed by 48 h in LL (gray) or DD (black). Data are from three independent experiments ± SE. C, Immunodetection of CrDOF in a purified recombinant protein fraction (Rec; 1 μg) and algal crude extract (Native; 50 μg). Black lines are MM markers in kD. D, CrDOF protein levels in CW15 in a 24-h course in LD (solid line) and SD (dashed line). Data are from two independent experiments ± SE. *, $P < 0.05$. E, Confocal images of CW15 and *CrDOF*ox:YFP lines. SYTOBlue45 fluorescence around nuclear regions (blue), YFP (yellow), chloroplast (red) are shown. Bars = 5 μm.

reflected an SDS-resistant posttranslational modification, such as has been shown for other SDS-resistant complexes from plants and animals described previously in the literature (Lüders et al., 2003; Varet et al., 2003; Kubista et al., 2004). Using these antibodies, we followed the presence of CrDOF in 24-h courses in LD and SD (Fig. 2D; Supplemental Fig. S1A) in protein extracts from the same samples as in Figure 2A. CrDOF protein showed a higher accumulation in LD than in SD and a clear circadian oscillation. However, in contrast to the mRNA profile, CrDOF minimal presence was monitored at ZT4 and its maximum was monitored at dusk (ZT16–20), coinciding with the CDF2 stability profile in Arabidopsis (Fornara et al., 2009). Thus, the expression of *CrDOF* mRNA and its protein stability are displaced in time.

To study CrDOF modifications, protein extracts from *C. reinhardtii* were incubated with different chemicals and immunodetected with α-CrDOF. When proteins were extracted with 8 M urea (a potent chaotropic agent) or in the presence of 10 mM dithiothreitol (DTT; which breaks Cys disulfide bonds) or a mixture of both (Supplemental Fig. S1B, top), only the 100-kD band was detected. Nevertheless, when proteins were extracted with a buffer containing 6 M guanidine chlorhydrate, a potent ionic chaotrop, the band of 100 kD was replaced by a band of 60 kD (Supplemental Fig. S1B, right). To discard ubiquitin modifications that are involved in Arabidopsis CDF stability (Imaizumi et al., 2005), extracts were incubated with 1 mM of the proteasome inhibitor MG-132. However, the intensity of the signal of the 100-kD band did not increase or show any mobility shift (Supplemental Fig. S1B, bottom right), probably indicating that the proteasome was not involved in CrDOF stability. Therefore, it is possible that CrDOF establishes tight connections with other proteins that control its function. As CDF stability is reduced under blue light in Arabidopsis (Imaizumi et al., 2005), we monitored if CrDOF stability was influenced by light quality. *C. reinhardtii* cultures were grown under LL, DD, constant blue light, or constant red light, cell extracts were prepared, and immunoblots were run using CrDOF antibodies. No significant difference in CrDOF accumulation was detected in any light condition (Supplemental Fig. S1C), indicating that light quality has no effect on its posttranslational stability.

The presence of CrDOF protein was also monitored using the confocal microscope in an algal line (*CrDOF*ox:YFP; see below) that expressed the yellow fluorescent protein fused to the CrDOF C-terminal end (Fig. 2E). To identify the cell nucleus, we developed a novel method for *C. reinhardtii* using the nucleic acid-specific dye SYTOBlue45 (Molecular Probes) in order to visualize nuclear material in vivo without interfering with YFP and chloroplast fluorescence (see "Materials and Methods"). SYTOBlue45 dyes in blue a nucleic acid-rich region of CW15, sited in the flagella pole and encircled by the unique cup-shaped structure of the chloroplast, which we identified as the nucleus (Fig. 2E, top). The merged image in the bottom row of Figure 2E shows that the YFP signal coincided with the blue signal from the dye, indicating that the CrDOF:YFP fusion was preferentially localized in the nucleus.

Modification of *CrDOF* Expression Alters *C. reinhardtii* Growth

To clarify the role of *CrDOF* in *C. reinhardtii*, algal lines with altered levels of *CrDOF* mRNA were produced using Gateway technology vectors (Invitrogen) containing constitutive or inducible promoters (see "Materials and Methods"). Thus, *CrDOF* genomic sequence was fused to the pnia2 promoter (*CrDOF*in) for inducible expression depending on the nitrogen source (Camargo et al., 2007). Figure 3A, top left, shows that *CrDOF* expression was significantly increased in CW15 transformed with the *CrDOF*in construct under inductive ($+NO_3^-$) conditions, also detecting an increase in protein levels by western blots (Fig. 3A, bottom left). *CrDOF* expression levels increased when *CrDOF* was fused to YFP in its C-terminal end and expressed under the control of the chimeric promoter HEAT SHOCK PROTEIN70/RIBULOSE BISPHOSPHATE CARBOXILASE-OXYGENASE SMALL SUBUNIT2 (RbcS2; *CrDOF*ox:YFP) for constitutive expression (Sizova et al., 2001; Fig. 3A, top right). Extracts from these algae presented an extra 120-kD band corresponding to the MM of CrDOF plus the YFP protein (Fig. 3A, bottom right, arrow). *CrDOF* expression was significantly reduced employing an artificial microRNA (*amiCrDOF*; see "Materials and Methods") strategy (Molnar et al., 2009) that was reflected in a decrease in mRNA and protein levels in extracts from the two independent silenced lines (*amiCrDOF* #1 and #4; Fig. 3B). *CrDOF* overexpression from the constitutive and the induced promoters had a strong effect on algal growth (Fig. 3C, left). Wild-type and recombinant culture growth in liquid medium (Sueoka NO_3^-; see "Materials and Methods") was monitored by measuring chlorophyll content during 4 weeks in LD. Whereas CW15 reached the exponential growth phase in week 2, it was retarded in week 3 in the *CrDOF*ox:YFP line and even further in the *CrDOF*in line. The *amiCrDOF* #1 and #4 cultures also grew slower than the CC-4351 wild type (Fig. 3C, right). The growing capacity of the lines was further measured in LD and SD, both on rich (Tris-acetate-phosphate [TAP] NO_3^-) and normal (Sueoka NO_3^-) medium agar plates, by droplet growth monitoring (Supplemental Fig. S1D). In all conditions, decreasing or increasing *CrDOF* transcript levels slowed algal growth, indicating that changes in *CrDOF* levels affected the growing conditions of the algae.

To assess the systemic effect of *CrDOF* overexpression in *C. reinhardtii*, a transcriptomic approach was used. *C. reinhardtii* cells (CW15) and two overexpression lines (*CrDOF*in and *CrDOF*ox:YFP) were grown in Sueoka NO_3^- medium in LD and SD, and RNA was extracted at ZT4 and sequenced using the NGS platform Illumina

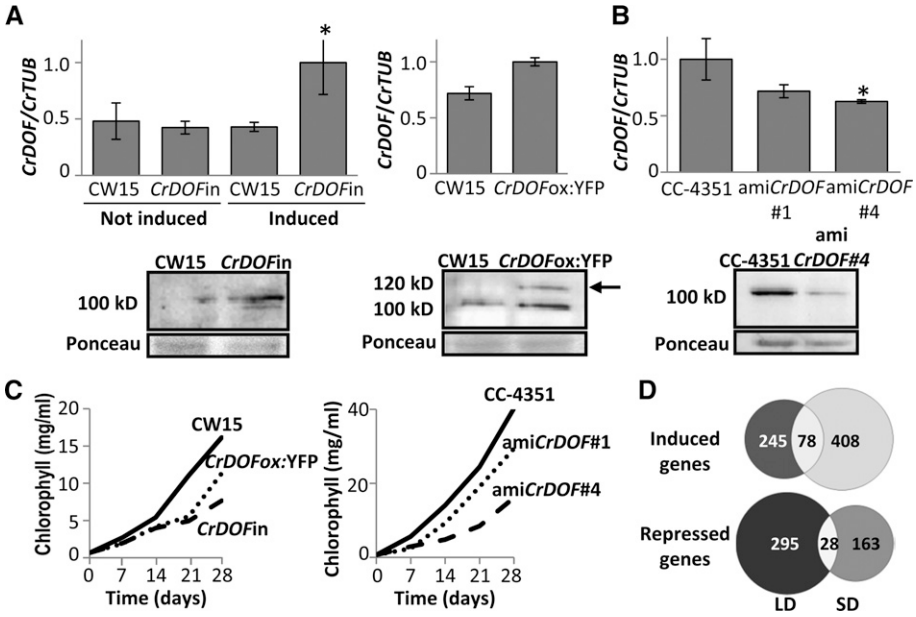

Figure 3. Altering *CrDOF* expression affects algal growth. A, *CrDOF* transcript levels (graphs at top) and protein (immunoblots at bottom) in CW15 and *CrDOF*in before and after 2 h of induction and *CrDOF*ox:YFP lines at ZT4 in LD. The arrow marks the 120-kD band corresponding to the CrDOF:YFP fusion. B, Reduction in *CrDOF* transcript levels (graphs at top) and protein (immunoblots at bottom) in *amiCrDOF* #1 and #4 compared with CC-4351 at ZT4 in LD. *, $P < 0.05$. C, Growth curves (chlorophyll content) in CW15 (solid line), *CrDOF*in (dashed line), and *CrDOF*ox:YFP (dotted line) at left and CC-4351 (solid line), *amiCrDOF* #1 (dotted line), and *amiCrDOF* #4 (dashed line) at right in a 4-week course. D, Venn diagrams for induced (top) or repressed (bottom) genes from the RNAseq data comparing CW15 and the intersection between *CrDOF*ox:YFP and *CrDOF*in lines (Supplemental Fig. S1E) in LD (left) and SD (right).

HiSeq 2000. After all quality parameters were verified, a stepwise protocol to analyze the transcriptome, using the *C. reinhardtii* genome as reference, was run (see "Materials and Methods"). Several software tools for read mapping (Bowtie and TopHat), transcriptome assembly (Cuffmerge and Cufflinks), and differential gene expression analysis (Cuffdiff and CummeRbund) were used. Differentially expressed genes between CW15 and the two overexpression lines were identified, and Venn diagrams representing these differences were drawn (Supplemental Fig. S1E). The RNAseq data analysis showed that *CrDOF* overexpression in both lines affected the expression of thousands of genes: 2,399 genes induced and 2,431 repressed in *CrDOF*in and 3,255 genes induced and 2,632 repressed in *CrDOF*ox:YFP in both LD and SD. When we separately analyzed the intersection between induced and repressed genes of both overexpression lines compared with the wild type in LD and SD and created Venn diagrams (Fig. 3D), a tendency in gene expression, which was daylength dependent, emerged. *CrDOF* overexpression caused the specific induction of 245 genes in LD and 408 genes in SD, while it caused the specific repression on 295 genes in LD and 163 genes in SD. Therefore, the RNAseq data from the two independent overexpression lines indicated that *CrDOF* would function preferentially as a repressor of gene expression in LD and as an inducer in SD. These data can be further analyzed on the Web page http://viridiplantae.ibvf.csic.es/crdof_cell_cycle.html.

CrDOF Induces *CrCO* Expression in *C. reinhardtii*

In Arabidopsis and potato (*Solanum tuberosum*), CDFs reduce *CO* expression and delay flowering (Imaizumi et al., 2005; Fornara et al., 2009; Kloosterman et al., 2013). To show that CrDOF could have a similar role in algae, *CrCO* expression was monitored in 24-h experiments in CW15, *CrDOF*in, and *CrDOF*ox:YFP lines (Fig. 4A). Both in LD and SD, *CrDOF*in and *CrDOF*ox:YFP showed an increase in *CrCO* expression during the morning and night. This was also observed in experiments in which *CrDOF*in lines were transferred from not induced (Supplemental Fig. S2A, left) to induced (Supplemental Fig. S2A, right) conditions for 2 h, resulting in a 3-fold increase in *CrCO* expression. Constitutive *CrDOF*ox:YFP lines that presented a moderate activation of *CrDOF* expression also showed a moderate increase in *CrCO* expression (Supplemental Fig. S2B). On the contrary, in *amiCrDOF* #1 and #4 (Fig. 4B), reduced levels of *CrDOF* produced a reduction in *CrCO* mRNA levels. Thus, both incrementing and reducing *CrDOF* expression levels had a parallel effect on *CrCO*, but rather than inhibiting *CO* expression, as in

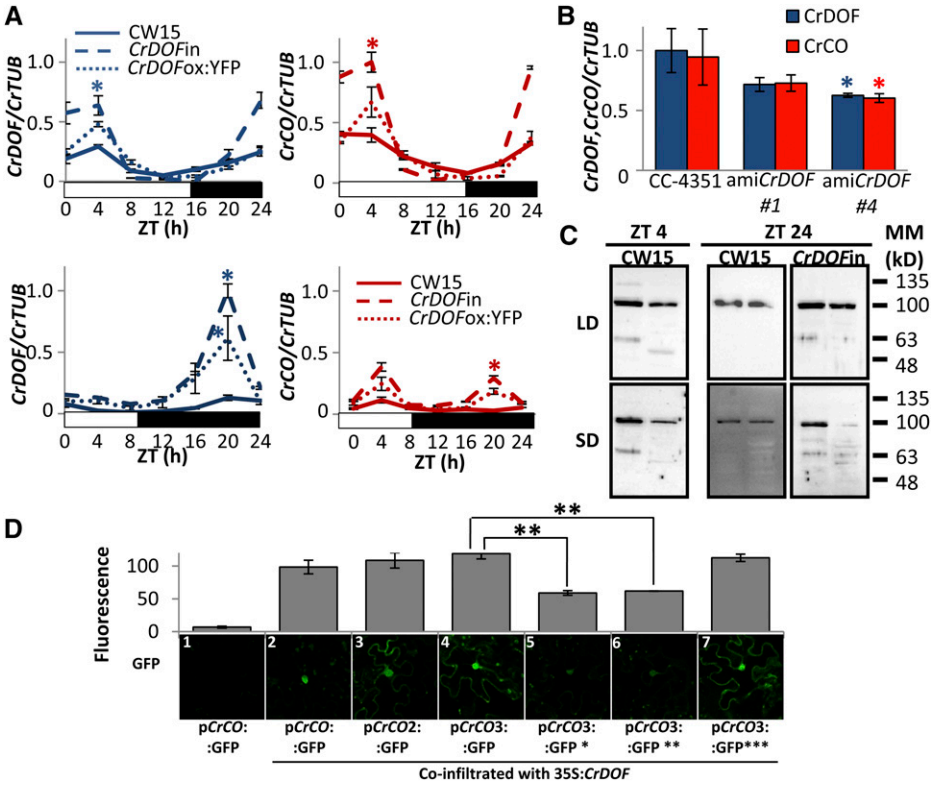

Figure 4. CrDOF induces *CrCO* expression. A, A 24-h course of CrDOF (blue) and *CrCO* (red) expression in LD (top) or SD (bottom) in CW15 (solid lines), *CrDOF*in (dashed lines), and CrDOFox:YFP (dotted lines). B, Levels of *CrDOF* (blue columns) and *CrCO* (red columns) mRNA in CC-4351 and *amiCrDOF* #1 and #4. Data are from three independent experiments ± SE. C, Immunodetection of CrDOF with α-CrDOF in gel filtration fractions 8 (464 kD; left) and 9 (314 kD; right) in protein extracts from cultures in LD (top) or SD (bottom). CW15 at ZT4 (left) and both CW15 and *CrDOF*in at ZT24 (right) are shown. Black lines are MM markers in kD. D, GFP fluorescence measurements (top) of different p*CrCO*:GFP constructs in *N. benthamiana* cells coinfiltrated with 35S:*CrDOF*. Data are from 100 nuclei in three independent experiments ± SE. Results from a significant experiment are shown below each graphic. *, $P < 0.05$; **, $P < 0.01$.

Arabidopsis, *CrDOF* behaved as an activator of *CrCO* expression in *C. reinhardtii*.

As we had observed 60- and 100-kD CrDOF protein bands on *C. reinhardtii* immunoblots, we wondered if this had a biological significance, so we performed gel filtration experiments in a Superose 12 10/300 GL (GE Healthcare) column attached to an FPLC device (GE Healthcare). Total extracts from CW15 or *CrDOF*in lines in LD and SD at ZT4 and ZT24 were run in the column, and the elution profile was separated by size and monitored for CrDOF presence (Fig. 4C; Supplemental Table S2). In CW15, a protein complex containing CrDOF eluted only in two fractions corresponding to MM of 464 and 314 kD (Supplemental Fig. S2, C and D). The 100-kD band was observed in all conditions, but the 60-kD protein was only detected at ZT4 in the fraction with the higher MM complex (Fig. 4C). At ZT24, the 60-kD band was absent in CW15 but was present in the *CrDOF*in extract in both fractions. Because *CrCO* expression in wild-type cells reaches its highest peak at ZT4 and in *CrDOF*in is induced at ZT24, we think that this correlates well with the 60-kD band representing the free, active protein that is able to modify *CrCO* expression. Moreover, the ratio between CrDOF and partners seems to have an important role in the complex size, as the 60-kD band presence always coincided with the higher MM complex.

The capacity to interact with itself was also investigated by bimolecular fluorescence complementation (BiFC; Supplemental Fig. S3A). A translational fusion of CrDOF to the YFP N-terminal part (YFN-CrDOF) was coinfected by *Agrobacterium tumefaciens*-mediated infiltration in *Nicotiana benthamiana* leaves together with CrDOF fused to the C-terminal part of the YFP (YFC-CrDOF). The presence of a strong yellow signal in the nucleus of the coinfiltrated *N. benthamiana* cells showed that CrDOF was able to interact with itself to form dimers or higher MM complexes.

To test if *CrDOF* could bind to the *CrCO* promoter, *A. tumefaciens*-mediated coinfiltration experiments were run. The sequence (846 bp) expanding the intergenic region between *CrCO* and the upstream gene (Cre06.g278158; Supplemental Fig. S3B) was cloned before the GFP coding sequence in a plant transformation vector (p*CrCO*:GFP). This construct did not show any expression in *N. benthamiana* cells using the confocal microscope (Fig. 4D, image 1), indicating that no plant factor could bind to the *C. reinhardtii CrCO* promoter. When a construct overexpressing *CrDOF* under the control of a plant constitutive promoter (35S:*CrDOF*) was coinfiltrated with p*CrCO*:GFP, a marked increase in GFP fluorescence was observed (Fig. 4D, image 2), demonstrating that CrDOF could bind to the *CrCO* promoter. In order to quantify the signal, more than 100 nuclei were monitored using the confocal microscope and their fluorescence registered (representing 100% signal). To identify the minimal promoter that still showed CrDOF binding, a 527-bp fragment of p*CrCO*2 (underlined in Supplemental Fig. S3B) and a 285-bp fragment of p*CrCO*3 (blue in Supplemental Fig. S3B) were cloned before the GFP coding sequence and coinfiltrated with the 35S:*CrDOF* construct in *N. benthamiana* leaves. As observed in Figure 4D (images 3 and 4), GFP

fluorescence did not decrease, indicating that the minimal promoter p*CrCO*3 contained all sequences needed for CrDOF binding. In the 285-bp fragment, three canonical DOF AAAG-binding sites were found (gray in Supplemental Fig. S3B). The three motifs were mutated individually to confer p*CrCO*3:GFP*, p*CrCO*3:GFP**, and p*CrCO*3:GFP*** constructs (Supplemental Fig. S3B). Only p*CrCO*3:GFP* and p*CrCO*3:GFP** showed significant decreases in GFP fluorescence when coinfiltrated with 35S:*CrDOF*, indicating that the motif closer to the *CrCO* initial ATG codon was not involved in CrDOF binding (Fig. 4D, images 5–7). The two elements with positive binding activity conserved the (A/T)AAAG or (A)CTTT(A) extra nucleotides characteristic of DOF-binding sites (Yanagisawa and Schmidt, 1999) not present in the third site. Therefore, we identified the binding site sequence of the primitive *DOF* gene and showed that it recognized the same core region as in higher plants. This constitutes additional evidence of the conservation of DOF TF function during plant diversification.

CrDOF Alters Algal Cell Cycle Progression in a Photoperiod-Dependent Manner

CrCO misexpression was shown to affect synchronous division in *C. reinhardtii* and, thus, the capacity to synchronize cell division and growth in particular environmental and photoperiod conditions (Serrano et al., 2009). As *CrDOF* overexpression and artificial microRNA constructs showed growth defects and altered *CrCO* expression, we examined if the cell cycle was also affected in these lines. Cell cycle defects are associated with changes in size due to cell division alterations (Umen and Goodenough, 2001). When we analyzed *CrDOF*in and *CrDOF*ox:YFP cells in LD by flow cytometry (Fig. 5A, top), they showed an increase in size compared with CW15, whereas in SD they were smaller. On the contrary, *amiCrDOF* #1 and #4 lines did not show any significant alteration in cell size in LD but showed a marked decrease in SD. Therefore, cell size in *C. reinhardtii* was severely affected by changes in *CrDOF* expression and was influenced by photoperiod.

Cyclins and cyclin-dependent kinases are key proteins involved in cell cycle progression in eukaryotes, and this function is conserved in green microalgae (Bisova et al., 2005). In *C. reinhardtii*, it was shown that *Cyclin A1* (*CrCYCA1*) and *Cyclin-dependent kinase B1* (*CrCDKB1*) transcript levels increased when *CrCO* levels increased in SD in order to promote the highly synchronized mitotic divisions at the end of the day characteristic of synchronous growth (Serrano et al., 2009). In order to assess the role of CrDOF in this process, we measured the capacity to activate the expression of *CrCYCA1* and *CrCDKB1* in LD and SD in the inducible line. *CrDOF* induction in two independent lines greatly enhanced the expression of *CrCYCA1* in SD (Fig. 5B, bottom left), while in LD it had the opposite effect (Fig. 5B, top left), inhibiting the small peak of expression present in CW15. *CrCDKB1* expression showed a similar response, as it was significantly enhanced in SD but was strongly inhibited in LD by *CrDOF* overexpression (Fig. 5B, right). Therefore, *CrDOF* overexpression altered cell cycle progression by increasing *CrCYCA1* and *CrCDKB1* transcript levels in SD and decreasing them in LD. Because *CrDOF* activates *CrCO* expression, this effect may be associated with the induction in *CrCO* mRNA levels observed in *CrDOF*in during the morning (Fig. 4A), but this could not explain the inhibitory effect in LD. To confirm these results, we performed a clustering and functional enrichment using the RNAseq data from CW15, *CrDOF*in, and *CrDOF*ox:YFP lines in SD and LD at ZT4. The functional enrichment of genes inhibited by *CrDOF* overexpression in LD showed that a significant part of the genes were involved in cell cycle progression, including *CrCYCA1* and *CrCDKB1* (http://viridiplantae.ibvf.csic.es/crdof_cell_cycle.html). Therefore, *CrDOF* inhibits cell cycle progression in LD

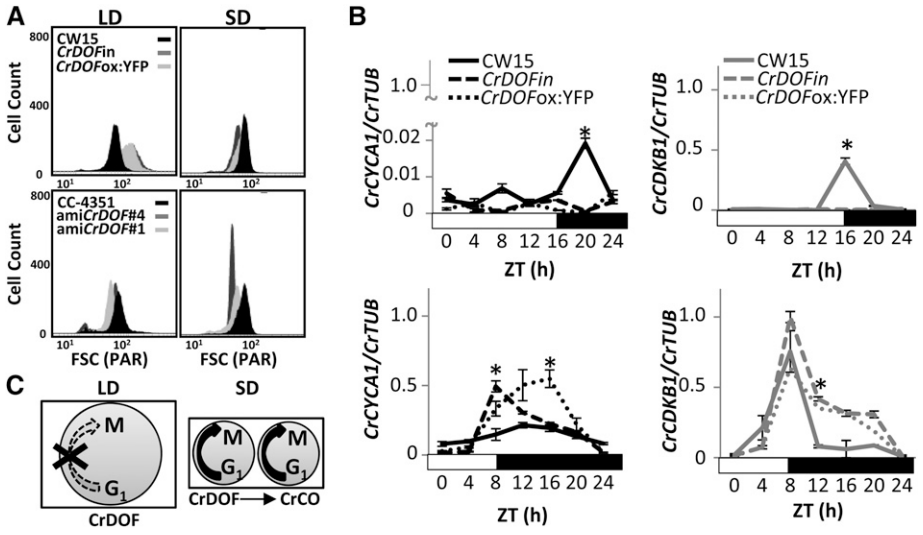

Figure 5. CrDOF controls the *C. reinhardtii* cell cycle. A, Flow cytometer cell size from algal cultures in LD (left) and SD (right) in CW15 (black), *CrDOF*in (dark gray), and *CrDOF*ox:YFP (light gray) at top or CC-4351 (black), *amiCrDOF* #4 (dark gray), and *amiCrDOF* #1 (light gray) at bottom. B, Expression of *CrCYCA1* (black) and *CrCDKB1* (gray) in LD (top) and SD (bottom) in CW15 (solid lines), *CrDOF*in (dashed lines), and *CrDOF*ox:YFP (dotted lines) in 24-h courses. Data are from three independent experiments ± SE. *, $P < 0.05$. C, Scheme of CrDOF control over cell cycle progression in LD (left) and SD (right). Circle size represents algal size, and number of circles represents growth progression.

independently of *CrCO* and activates its progression in SD by inducing *CrCO* expression (Fig. 5C). In this scenario, cells would be larger in LD, as the cell cycle is inhibited during the day (Fig. 5C, left), while in SD cells maintain a small size due to the activation of the cell cycle promoted by *CrCO* (Fig. 5C, right), as we had shown previously in the flow cytometer experiments.

CrDOF in Arabidopsis Delays Flowering through the Interaction with CDFs

In Arabidopsis, CDFs inhibit *CO* expression during the morning to avoid *FT* misexpression outside the evening coincidence window that sets the exact synchronization of flowering by daylength. To test the capacity of *CrDOF* to alter flowering time in Arabidopsis, we expressed *CrDOF* under the control of the constitutive promoter 35S (35S:*CrDOF*). *CrDOF* heterologous expression in Arabidopsis delayed flowering in LD, 35S:*CrDOF* plants flowering with 10 leaves more than Columbia-0 (Col-0), and had no effect in SD (Fig. 6A; Table I). We then followed *CO* and *FT* expression during a 24-h course in LD (Fig. 6B) and SD (Supplemental Fig. S4A) in Col-0 and 35S:*CrDOF* plants. While *CO* expression was reduced during the daytime in LD, particularly during the evening (shadowed in Fig. 6B, left), the expression in SD was not affected (Supplemental Fig. S4A, top). In 35S:*CrDOF* plants in LD, *FT* expression was strongly inhibited during the whole photoperiod (Fig. 6B, right), explaining the late-flowering phenotype in LD, but in SD no effect was observed (Supplemental Fig. S4A, bottom).

CDFs work additively to repress *CO* and *FT* expression, so that in the quadruple mutant *cdf1/cdf2/cdf3/cdf5* (*4cdf*), *CO* transcript levels are constitutively high (Fornara et al., 2009). We tested if *CrDOF* could complement the early-flowering phenotype observed in *4cdf* (Fig. 6C; Table I). While the *4cdf* mutant flowered earlier than Col-0 in LD and SD, ectopic expression of *CrDOF* in the *4cdf* background had no effect on flowering time. Therefore, *CrDOF* had no effect on the floral transition in the absence of CDFs. This suggests that CrDOF may interact with the CDFs and enhance their capacity to inhibit *CO* and *FT* expression. To test this hypothesis, we performed BiFC experiments in *N. benthamiana* (Supplemental Fig. S4B). Both CDF1 and CDF2 were able to interact with each other and CDF2 with itself (Supplemental Fig. S4B, images 3 and 4), but they could also interact with CrDOF (Supplemental Fig. S4B, images 1 and 2). When we used CrDOF-specific antibodies in Col-0 nuclear extracts, we could detect several bands around and below 60 kD that could account for Arabidopsis DOF TFs, including CDFs, which present smaller size than other DOFs (Supplemental Fig. S4C, left). In fact, these signals increased in extracts from ZT0 to ZT8, where the maximum amount of CDFs is supposed to accumulate (Fornara et al., 2009). In 35S:*CrDOF* plants, the immunodetection of the 60-kD band increased significantly both in Col-0 and in the *4cdf* mutant background (Supplemental Fig. S4C, right), due to the accumulation of CrDOF, but we could never detect the 100-kD band that we had observed in *C. reinhardtii*.

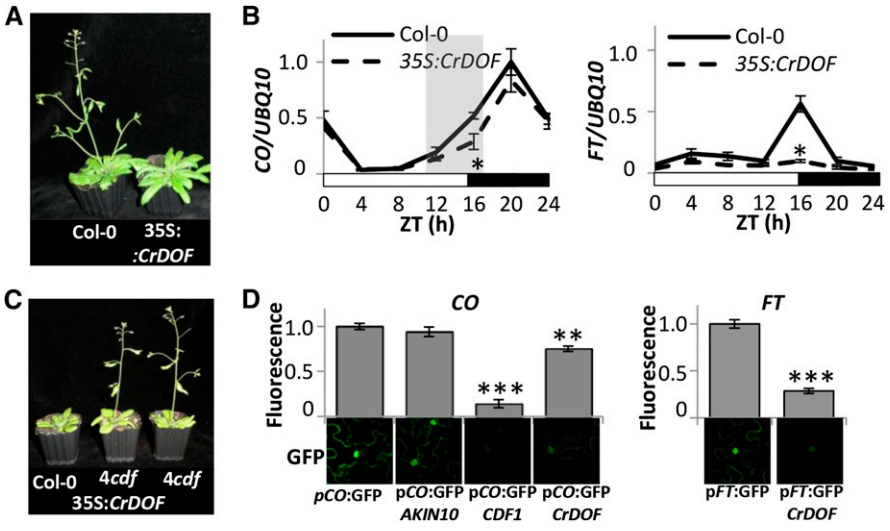

Figure 6. *CrDOF* expression delays flowering in Arabidopsis. A, Late-flowering phenotypes of Arabidopsis 3-week-old plants in LD expressing *CrDOF* under the control of the 35S promoter (right) compared with Col-0 (left). B, *CO* and *FT* 24-h mRNA levels in Col-0 and 35S:*CrDOF* from 14-d-old plants in LD. Data are from three independent experiments ± SE. C, Flowering phenotypes of *4cdf* (right), *35S:CrDOF 4cdf* (middle), and Col-0 (left) plants grown in soil for 2 weeks in LD. D, Confocal images of 35S:*CrDOF*-infiltrated *N. benthamiana* cells together with *CO* (left) or *FT* (right) promoter fused to GFP are shown at bottom. *CDF1* (positive) and *AKIN10* (negative) coinfiltrations were used as controls. GFP fluorescence quantifications are shown at top. Data are from 100 nuclei in three independent experiments ± SE. *, $P < 0.05$; **, $P < 0.01$; ***, $P < 0.001$.

Table I. *Flowering time of Col-0, mutants, and 35S:CrDOF plants in LD and SD*

Data are shown as means ± SE of 30 plants from three independent experiments scored for total leaf number at the moment of appearance of the floral bud in LD and SD. Transgenic lines described in this work are T3 plants. $^{**}P < 0.01$ by Student's *t* test.

Plant	LD	SD
Col-0	20.45 ± 1.2	66.7 ± 4.4
35S:CrDOF	30.54 ± 2.2**	65.62 ± 4.7
4cdf	11.26 ± 0.93	14.42 ± 1.54
35S:*CrDOF 4cdf*	11.05 ± 0.41	14.45 ± 2.05

The exclusive presence of the 60-kD band in the recombinant *E. coli* cultures (Fig. 2C), the detection of the 60- and 100-kD bands in the gel filtration experiments in *C. reinhardtii* (Fig. 4C), and the lack of a 100-kD band in Arabidopsis strongly suggest that the higher MM must be a specific characteristic of algae DOFs and that the active form must be the 60-kD protein. Using a 35S:*GFP*:*CrDOF* construct, we could also show the nuclear localization of CrDOF in Arabidopsis (Supplemental Fig. S4D).

To further demonstrate the effect of CrDOF over *CO* and *FT* expression, we infiltrated *N. benthamiana* cells with *A. tumefaciens* carrying constructs expressing *GFP* under the control of the *CO* (p*CO*:*GFP*) and *FT* (p*FT*:*GFP*) promoters (Fig. 6D). Both constructs showed a clear nuclear GFP signal when infiltrated alone. When a negative control (*AKIN10*) was cotransformed with p*CO*:*GFP*, no reduction in GFP fluorescence was observed. As expected, cotransformation of p*CO*:*GFP* with a construct ectopically expressing *CDF1* produced a dramatic decrease in GFP fluorescence. Ectopic coexpression of *CrDOF* had a lower, but still significant, effect in GFP fluorescence. In a similar way to what was shown in the expression experiments, CrDOF also reduced GFP fluorescence when GFP was driven by the *FT* promoter (Fig. 6D, right), suggesting a role for CrDOF (and CDFs) in *FT* expression.

DISCUSSION

DOF proteins are present in the genomes of higher plants and unicellular green algae (chlorophytes) and are absent from all other algal divisions and, in fact, from any other prokaryote or non-green-lineage eukaryote (Moreno-Risueno et al., 2007). This way, we could identify CrDOF sequences in several chlorophyte orders, such as Chamydomonadales (*C. reinhardtii* and *Volvox* spp.), Trebouxiophyceae (*Chlorella* and *Coccomyxa* spp.), Mamiellales (*Ostreococcus*, *Bathyococcus*, and *Micromonas* spp.), and Chlorodendrales (*Tetraselmis* spp.). CrDOF sequences were absent from other major algal divisions, such as the primary endosymbionts rhodophytes (*Cyanidioschyzon* spp.) and glaucophytes (*Cyanophora* spp.), but also from other secondary endosymbionts, such as euglenophytes (*Euglena* spp.), haptophytes (*Emiliania* spp.), heteroconts (*Phaeodactylum*, *Thalassiosira*, and *Navicula* spp.), cryptophytes (*Guillardia* spp.), chloraracniophytes (*Bigelowiella* spp.), and dynophytes (*Symbiodinium* spp.). Therefore, they constitute a good model to study the evolution of specific regulatory pathways in plants. *DOFs* are found as single-copy genes in the genome of chlorophytes, but in *P. patens*, we have identified 16 genes homologous to *CrDOF*, while others have identified a family of 19 members (Shigyo et al., 2007). In rice and maize, around 31 and 10 *DOF* genes have been identified, respectively, while in Arabidopsis and *Populus* spp., the numbers are even higher: 36 and 61, respectively (Noguero et al., 2013). Therefore, this family has increased from a single-copy gene in algae to a multicopy family with numerous functions, including the control of photoperiodic flowering, in angiosperms. Therefore, the study of the ancestral function of the algal DOF was important to understand how different regulatory pathways are controlled, being the photoperiod pathway of special interest.

In Arabidopsis, potato, and rice, several *DOF* genes have been classified as *CDFs* because they are regulated by the clock and at the same time regulate photoperiodic flowering (Imaizumi et al., 2005; Fornara et al., 2009; Li et al., 2009; Kloosterman et al., 2013). In its domain structure, ancient DOF proteins contained a single DOF domain with an NLS in its N-terminal part. This structure is repeatedly found in green microalgae. In the course of evolution, as observed in *P. patens* DOFs, different domains were incorporated to the basic pattern that added new regulatory elements to the protein and recruited novel regulators to the pathway (Fig. 1C). As a culmination to this evolutionary process, higher plant CDFs possess an established structure that is the combination of several domains present in bryophytes, such as the GI- and FKF1-binding elements, responsible for their complex posttranslational regulation. Therefore, the evolution of DOF factors is a good example of the innovation-amplification-divergence model of evolution by gene duplication described also for the family of *COL* genes in photosynthetic eukaryotes (Romero-Campero et al., 2013).

DOF TFs have multiple roles in plants, from the control of nitrogen and carbon metabolic balance, as in maize *DOF1* (Yanagisawa, 2000), to the control of photoperiodic flowering by Arabidopsis *CDFs* (Imaizumi et al., 2005; Fornara et al., 2009). At the molecular level, they function as DNA-binding proteins that regulate transcription, either inducing or repressing gene expression (Noguero et al., 2013). Here, we have shown that the *C. reinhardtii* single-copy *DOF* gene already had this double function. We provide evidence for gene induction at the individual level, such as *CrCO* or the repression of *CrCYCA1* and *CrCDKB1* in *CrDOF* overexpression lines, but we also provide systemic-level evidence using RNAseq data from wild-type and *CrDOF* overexpression lines under different photoperiod conditions. We have further shown that CrDOF preferentially induces or represses gene

expression depending on photoperiod, such that it is mainly an activator of gene expression in SD and an inhibitor in LD. Indeed, both functions can be recruited to achieve the same goal, such as the regulation of synchronous growth. In *C. reinhardtii* and other microalgae, cell division is synchronized to the cell cycle (Bišová and Zachleder, 2014), and this is affected by daylength. This way, in LD or LL, with an excess of resources, algae can divide several times and no peak in cell cycle genes is detected. On the contrary, in SD, in stress conditions or nutrient limitation, algae divide once a day and the cell cycle genes peak at dusk (Serrano et al., 2009). Therefore, we can now compare CrDOF overexpression line data with *CrCO* transgenic line data (Serrano et al., 2009), where CrCO positively regulated *CrCYCA1* and *CrCDKB1* transcript levels in SD conditions. Thus, we propose that CrDOF induces *CrCO* expression in SD at the end of the day, promoting the up-regulation of cell cycle factors such as *CrCYCA1* and *CrCDKB1* (Fig. 7). This peak of expression activates the cell cycle and ensures cell division in that particular time, allowing all algae in the culture to divide synchronously. In LD, on the contrary, CrDOF inhibits the expression of cell cycle genes in specific conditions when no synchronous division is necessary, thus allowing indeterminate cell division throughout the day. In fact, in Arabidopsis, the DOF factor *OBF BINDING PROTEIN1* is involved in the control of the cell cycle by inducing the expression of the cyclin *CYCD3.3*, and its overexpression causes the reduction of G1 phase, accelerating growth (Skirycz et al., 2008), suggesting that this algal DOF function is conserved in plants.

Our data suggest that a posttranslational regulatory step is necessary to explain CrDOF function, as CrDOF can bind to DNA as a single 60-kD form, but it is mostly detected as a 100-kD band in *C. reinhardtii* extracts. We propose that the most plausible explanation is that a partner, or more than one, may bind CrDOF in a protein complex. Bound CrDOF would be unable to promote or inhibit gene expression. In the CrDOF-induced line, this regulation is lost, probably due to an excess of CrDOF in the complex, so that free CrDOF could then activate *CrCO* expression. The experiments in *N. benthamiana* cells that show that CrDOF can bind directly to the *CrCO* promoter, the absence of the 100-kD band in plant immunodetection, and the data from the chromatographic experiments in *C. reinhardtii*, where the 60-kD band appears only when CrDOF induces *CrCO* expression, suggest that CrDOF is active whenever the 60-kD band is detected. Therefore, we propose that the *CrCO* mRNA level induction by CrDOF in algae is a direct effect caused by DOF binding to its promoter.

In Arabidopsis, *CrDOF* overexpression delays flowering by reducing *CO* and *FT* levels exclusively in LD and not in SD, reflecting a strict photoperiodic response. In our model, as CrDOF cannot alter flowering time in the *4cdf* mutant, it is possible that CrDOF could act in a complex with the CDFs, protecting them from the proteasome degradation triggered by GI-FKF, as CrDOF does not present the binding domains for these proteins (Fig. 7, right). In *N. benthamiana* experiments, CrDOF also inhibit *CO* and *FT* expression, probably through the interaction with the *N. benthamiana* CDF homologs. This association between CDFs and CrDOF could have interesting applications in plant biotechnology to modify flowering time.

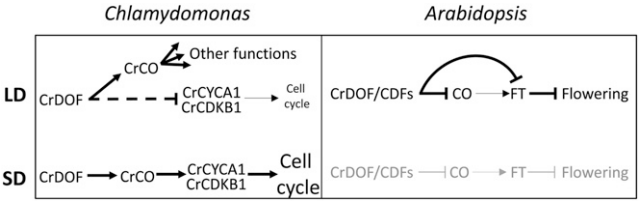

Figure 7. Model for CrDOF function in *C. reinhardtii* (left) and Arabidopsis (right). In *C. reinhardtii*, *CrDOF* in LD is able to induce *CrCO* expression by binding to its promoter and, moreover, slow down cell cycle progression by inhibiting, directly or indirectly (dashed T line), *CrCYCA1* and *CrCDKB1* expression. In SD, CrDOF induces cell cycle progression by promoting *CrCO* expression. In Arabidopsis, the CrDOF/CDF complex delays flowering time by inhibiting *CO* and *FT* expression in LD. In SD (gray), CO protein is not present and cannot induce *FT* expression, so *CrDOF* ectopic expression does not affect flowering time. Arrows indicate inductive actions, and T lines indicate inhibiting actions.

CONCLUSION

It is interesting that both *COL* and *DOF* genes seem to have suffered a similar evolutionary process and often cluster together in gene coexpression networks constructed from different organisms representing different steps of plant evolution (Romero-Campero et al., 2013). Both CO and CDF proteins are part of the photoperiod pathway. It is likely that other partners of this route (i.e. FLOWERING BASIC HELIX-LOOP-HELIX [Ito et al., 2012], FKF, and CONSTITUTIVE PHOTOMORPHOGENESIS PROTEIN1) followed a similar coevolution process. If this was the case and, further, could be demonstrated for other routes, it may constitute the basis of a general evolutionarily conserved process in which all members of a regulatory pathway (toolkit) evolve together, restrained and connected by the functional links established early in evolution in the original regulatory network (Romero-Campero et al., 2013; Della Pina et al., 2014; Ichihashi et al., 2014). Our demonstration that the DOF-CO module is conserved from algae to higher plants provides direct evidence that this effect may indeed be taking place. The study of these conserved toolkits throughout the plant evolutionary lineage may provide important hints to understand the processes that allowed the differentiation of higher plants from simple unicellular algae.

MATERIALS AND METHODS

Biological Material and Growth Conditions

Chlamydomonas reinhardtii wild types CW15 (Davies and Plaskitt, 1971) and CC-4351 (from René Matagne, University of Liège, via Michael Schroda, Max Planck Institute of Molecular Plant Physiology) and transgenic lines were grown in flasks with minimal Sueoka medium (Sueoka et al., 1967) or rich TAP medium (Harris, 1989) in LD or SD at 50-μE light intensity with temperatures ranging from 22°C (day) to 18°C (night). For induction of the *nia2* promoter, algal cells grown to exponential phase in Sueoka medium supplemented with ammonium were harvested by centrifugation (4 min at 3,200*g*) and suspended in Sueoka medium supplemented with nitrate.

Arabidopsis (*Arabidopsis thaliana*) plants were grown in soil for phenotypic analysis or in Murashige and Skoog agar medium supplemented with 1% (w/v) Suc plates for quantitative PCR (QPCR) assays. In both cases, seeds were previously incubated during 4 d at 4°C before sowing. Plants were grown in humidity-controlled (80%) chambers with a 100-μE light intensity and temperatures ranging from 22°C (day) to 18°C (night). Different photoperiods were used: 16 h of light/8 h of dark (LD) and 8 h of light/16 h of dark (SD).

Cloning and Analysis of *CrDOF*

The complete *CrDOF* ORF was obtained from the cDNA Collection of the Kazusa DNA Research Centre (http://www.kazusa.or.jp). Sequencing of the cDNA showed 100% identity with the predicted locus Cre12.g521150 (positions 4,425,725 to 4,430,320) from Phytozome version 9.1. The CrDOF deduced protein was 625 amino acids long and contained a DOF-type zinc finger domain (Yanagisawa, 1997; Moreno-Risueno et al., 2007).

Phylogenetic Analysis and Identification of Conserved Motifs

Evolutionary relationships among DOF proteins from the green algae *C. reinhardtii*, *Volvox carteri*, *Ostreococcus tauri*, and *Micromonas pusilla*, the bryophyte *Physcomitrella patens*, the monocots rice (*Oryza sativa*) and maize (*Zea mays*), and the dicots Arabidopsis and poplar (*Populus trichocarpa*) were analyzed using the CrDOF full-length amino acid sequence as a query to detect protein homologs in the Phytozome version 9.1 database. All sequences were aligned using the program MUSCLE (Edgar, 2004), and a phylogenetic tree was generated applying the neighbor-joining algorithm (Saitou and Nei, 1987) with the substitution model JTT + G 0.54 (Jones et al., 1992). The number of bootstrap replicates was 500. Phylogenetic analyses were conducted with MEGA5 (Tamura et al., 2011). Accession numbers of the sequences used in the alignment are shown in Supplemental Table S1. A domain analysis of the same 84 DOF proteins in the phylogenetic tree was done using the MEME software (http://meme.nbcr.net/meme/; Bailey et al., 2009). The motif domains were characterized using the Conserved Domain Search Service (http://www.ncbi.nlm.nih.gov/Structure/cdd/wrpsb.cgi). Further identification of the GI- and FKF1-binding domains was done as described (Kloosterman et al., 2013).

Phenotypic Analysis

Growth Curve and Drop Test

Algal cultures were grown to stationary phase in LD conditions and then diluted to 0.5 μg mL^{-1} chlorophyll with new medium. Culture growth was monitored by chlorophyll measurements once per week for 1 month. For drop tests, the culture in the stationary phase was diluted to 4 to 5 $\times$ 10^6 cells mL^{-1}, and three consecutive 1:10 dilutions were made. Three-microliter drops were grown on agar plates containing Sueoka NO_3^- or TAP NO_3^- medium and incubated in LD or SD.

Flow Cytometry

Wild-type and transgenic line samples were taken at ZT4 in LD and SD conditions in Sueoka medium supplemented with NO_3^- and analyzed on a BD Influx Cell Sorter flow cytometer (Becton Dickinson) equipped with a laser with a 488-nm line at 200 mW and analyzed with BD FACS software.

Analysis of Flowering Time

Flowering time was analyzed in LD and SD conditions in controlled-environment cabinets by scoring the number of rosette (excluding cotyledons) and cauline leaves. Data are from media of at least 30 individuals ± SE.

Algal and Plant Transformation

C. reinhardtii

For *C. reinhardtii* nuclear transformation, a modification of the electroporation protocol from Shimogawara et al. (1998) was used. In brief, about 1 to 5 $\times$ 10^6 cells mL^{-1} were harvested by centrifugation at 1,500*g* and suspended in TAP medium supplemented with 60 mM Suc in 1:100th of the original volume. A total of 250 μL of cell suspension and 1 μg of the plasmid were placed into a 0.4-cm gapped cuvette and incubated for 30 min on ice. After an 800-V pulse (15 μF and no shunt resistance) in an electroporator, cells were transferred to 10 mL of TAP medium supplemented with 60 mM Suc and incubated overnight with moderate shaking and light. Cells were harvested by centrifugation, resuspended in 700 μL of TAP medium, and spread into selective TAP agar plates containing hygromycin at 25 μg mL^{-1}. Colonies started to appear after 1 week. For the nitrate-inducible *CrDOF* expression vector construction, the Gateway-modified version of the pnia2 vector (Serrano et al., 2009) was used. For the constitutive *CrDOF* vector expression construction, direct gene synthesis from Invitrogen was used. In silico sequencing of the Hsp70A/RbcS2 constitutive promoter, Gateway cassette B, and the 3′-untranslated region of the Rubisco terminator was performed, and restriction enzyme sites present in the Gateway cassette and terminator were changed without modifying the codon use. YFP and hygromycin resistance were cloned into *Eco*RV/*Bam*HI and *Kpn*I restriction sites, respectively. YFP was adapted to the *C. reinhardtii* codon preference (Matsuo and Ishiura, 2010).

Arabidopsis

For Arabidopsis Col-0 or *4cdf* transformation, the *Agrobacterium tumefaciens*-mediated floral dip protocol was used. *CrDOF* cDNA was amplified by PCR (5′-GGGGACAAGTTTGTACAAAAAAGCAGGCTTCGAAGGAGATAGAACCATGGTAGACGGTGGTTCG-3′ and 5′-GGGGACCACTTTGTACAAGAAAGCTGGGTCTCACCTAGCACCCGAGTAAGC-3′ with stop codon and 5′-GGGGACCACTTTGTACAAGAAAGCTGGGTCCCTAGCACCCGAGTAAGCGGC-3′ without stop codon were used for C-terminal fusions) and cloned into the pDONOR 207 plasmid. Finally, *CrDOF* was cloned in the pEG100 vector to obtain the 35S:*CrDOF* construct and in the pMDC43 vector to obtain the 35S:GFP:*CrDOF* construct. Arabidopsis Col-0 plants were transformed with these constructs and plants selected for antibiotic resistance. The *4cdf* mutant plants were transformed with the 35S:*CrDOF* construct, and positive plants were selected by genome PCR tests using 5′-ACTGCAAGACGTGTCAGCG-3′ and 5′-GCCAACTCACTGTTGAACTGC-3′ primers.

RNA Techniques

Expression Analysis by QPCR

Total RNA from *C. reinhardtii* cells (20 mL of an exponential phase curve) or Arabidopsis seedlings (0.1 g of leaf tissue) was isolated by the Trizol (Invitrogen) procedure following the recommendations of the manufacturer. The final RNA sample was suspended in 30 μL of diethyl pyrocarbonate water, quantified in an ND-1000 spectrophotometer (Nanodrop), and stored at −80°C. One microgram of RNA was used to synthesize cDNA employing the QuantitecReverse Kit (Qiagen), diluted to a final concentration of 10 ng μL^{-1}, and stored at −20°C until QPCR was performed. Specific primers to amplify the 3′ region of each gene analyzed, plus *CrTUBULIN* and *UBIQUITIN10* (Supplemental Table S3) as housekeeping genes, were designed with the Oligo Analyzer program (Integrated DNA Technologies; www.idtdna.com). QPCR was performed with the iQTM5 Multicolor Real-Time PCR Detection System (Bio-Rad) in 10-μL reactions: primer concentration of 0.2 μM, 10 ng of cDNA, and 5-μL SensiFAST SYBR & Fluorescein Kit (Bioline). Each sample was measured in triplicate. The QPCR program consisted of (1) one cycle of 95°C for 2 min; (2) 40 cycles of 95°C for 5 s, 60°C for 10 s, and 72°C for 6 s; and (3) one cycle of 72°C for 6 s. Fluorescence was measured at the end of each extension step, and melting curve analysis was performed between 55°C and 95°C. The initial concentrations of candidate and reference genes were calculated by means of LingRegPCR software version 11.0 (Ruijter et al.,

2009). Normalized data were calculated by dividing the average of three replicates of each sample of the candidate and reference genes.

Transcriptomic Analysis by RNAseq

The experimental design consisted of two replicates for each genotype (*CrDOF*in, *CrDOF*ox:GFP, and wild-type CW15) and growth condition (LD and SD). RNA was extracted from each sample using Trizol. Library preparation was carried out following the manufacturer's recommendations. Sequencing of RNA libraries was performed with the Illumina HiSeq 2000 sequencer, yielding approximately 40 million 50-bp-long reads for each sample. The software package FastQC (Andrews, 2014) was used for quality control. All sequencing samples were of high quality, and no preprocessing of the reads was required to remove low-quality reads or read fragments. The *C. reinhardtii* reference genome version 5.3 (Merchant et al., 2007) and annotation were downloaded from the Phytozome database (Goodstein et al., 2012). Mapping of reads to the reference genome, transcript assembly, and differential expression were performed with the software tools Bowtie, TopHat, and Cufflinks (Trapnell et al., 2012) using default parameters. The R package from Bioconductor CummeRbund (Goff et al., 2012) was used for subsequent analysis and graphical representation of the results. Differentially expressed genes were selected as those exhibiting an expression fold change greater than 2 when compared with the wild-type CW15 and $P < 0.05$. Venn diagrams comparing the different sets of differentially expressed genes were generated with Venn Diagram Plotter (http://omics.pnl.gov/software/venn-diagram-plotter). The RNAseq raw data generated in this study are publicly available from the European Nucleotide Archive database identified with accession number PRJEB6682 (http://www.ebi.ac.uk/ena/data/view/PRJEB6682).

Protein and Immunological Techniques

Purification of Recombinant CrDOF

The *CrDOF* cDNA fragment was amplified by PCR using specific primers designed with *Nde*I/*Bam*HI restriction enzyme adaptors (5′-gggcatATGGTAGACGGTGGTTCGCGTG-3′ and 5′-cccggatccTCACCTAGCACCCGAGTAAGC-3′). The lower case portion of the sequences are three bases plus the restriction sequence (total or partial) introduced for PCR amplification and cloning. *CrDOF* was cloned into pET19b vector, which incorporates an N-terminal His tail (His-CrDOF), and transformed into *Escherichia coli* BL21 strain. Ten milliliters of an overnight culture of BL21 transformed with His-*CrDOF* was added to 1 L of Luria-Bertani medium containing 100 μg mL^{-1} ampicillin and grown at 30°C until the A_{600} reached 0.7. Recombinant gene expression was induced by the addition of 1 mM isopropylthio-β-galactoside and incubation during 4 h at 30°C. After centrifugation, the pellet was resuspended in lysis buffer (50 mM Tris-HCl, pH 8, 50 mM KCl, 1 mM EDTA, pH 8, 1 mM DTT, 10 mM $MgCl_2$, and 10% [v/v] glycerol) to 3 mL g^{-1} cells and broken by sonic disruption. After centrifugation, the pellet was solubilized with buffer IB (50 mM Tris-HCl, pH 8, 10 mM EDTA, pH 8, 0.5% [v/v] Triton X-100, and 0.1 mM phenylmethylsulfonyl fluoride [PMSF]), washed twice in the same buffer, and once with TALON K buffer (0.05 M phosphate buffer, pH 8, and 0.3 M KCl). Between each wash, the pellet was sonicated and centrifuged. Finally, the pellet was suspended in TALON buffer including 6 M guanidine chlorhydrate and incubated for 2 h. After this period, the protein extract was disrupted by sonication and centrifuged, and the supernatant was used to purify CrDOF employing BD TALON resin following the recommendations of the manufacturer in denaturing conditions (the presence of 6 M guanidine chlorhydrate). After elution, proteins were precipitated with 100% (v/v) ethanol for 30 min at 4°C. The pellet was washed twice (0.3 M guanidine chlorhydrate in 95% [v/v] ethanol and then 90% [v/v] ethanol). Finally, the pellet was suspended in SDS-PAGE buffer and separated by electrophoresis on 10% (w/v) polyacrylamide gels. One milligram of purified protein was used to produce antibodies.

Protein Extraction and Immunodetection

Cells from 20 mL of exponentially growing *C. reinhardtii* cultures were centrifuged and suspended in 3 mL g^{-1} extraction buffer (50 mM Tris-HCl, pH 7.5, 1 mM PMSF, 1 mM DTT, quimostatin, antipain, and leupeptin at 5 μg mL^{-1}, 10 mM β-mercaptoethanol, and 1:1,000 Sigma plant protease inhibitor cocktail). Algae were broken by two cycles of slow freezing to −80°C followed by thawing to room temperature. Cell extracts were centrifuged at 15,000*g* for 30 min at 4°C, and supernatant was collected. Protein content was estimated by the method of Bradford (1976) using ovalbumin as a standard. Samples were run on SDS-PAGE 10% (w/v) polyacrylamide gels and transferred to nitrocellulose membranes using the Trans-BlotTurboTransfer System (Bio-Rad) according to the manufacturer's instructions. Western-blot analysis was performed using specific antibodies raised against CrDOF recombinant protein. To disaggregate the CrDOF complex, total protein was processed by different treatments: 8 M urea, 0.1 M DTT, 8 M urea with 0.1 M DTT, and 6 M guanidine chlorhydrate.

Chromatography

Total protein from CW15 and *CrDOF*in cultures grown in Sueoka medium supplemented with NO_3^- at LD and SD was extracted as above. One milligram of protein was separated on a Superose 12 10/300 GL column (GE Healthcare). One-milliliter fractions were collected, precipitated with 10% (w/v) TCA, and run on SDS-PAGE gels. Western-blot analysis was performed using anti-CrDOF antibodies. Protein complex MM was calculated using the Gel Filtration Markers Kit (Sigma MWGF1000; Supplemental Fig. S2D).

Nuclear and Protein Extraction

Nuclear isolation of Col-0 and 35S:*CrDOF* (ZT0 and ZT8) was done as described (Lazaro et al., 2012). Protein extraction was carried out in native conditions using a high-salt buffer (1.6 M KCl, 50 mM HEPES, pH 8, 3 mM $MgCl_2$, 5 mM DTT, 1% [v/v] glycerol, and 1 mM PMSF) and run on SDS-PAGE gels. Western-blot analysis was performed using anti-CrDOF antibodies.

Transitory Expression in *Nicotiana benthamiana*

BiFC Experiments

To verify CrDOF protein interactions in vivo, *CrDOF*, *CDF1*, and *CDF2* complete ORFs were cloned in pYFN43 and pYFC43 to produce fusions to the YTP N-terminal part (YFN-CrDOF, YFN-CDF1, and YFN-CDF2) as well as to the YFP C-terminal part (YFC-CrDOF, YFC-CDF1, and YFC-CDF2). Specific primers were used for each gene (*CrDOF*, 5′-GGGGACAAGTTTGTACAAAAAAGCAGGCTTCGAAGGAGATAGAACCATGGTAGACGGTGGTTCG-3′ and 5′-GGGGACCACTTTGTACAAGAAAGCTGGGTCCCTAGCACCCGAGTAAGCGGC-3′; *CDF1*, 5′-GGGGACAAGTTTGTACAAAAAAGCAGGCTTCGAAGGAGATAGAACCATGCTGGAAACTAAAGATCCTGCG-3′ and 5′-GGGGACCACTTTGTACAAGAAAGCTGGGTCTCACATCTGCTCATGGAAATTGAT-3′; and *CDF2*, 5′-GGGGACAAGTTTGTACAAAAAAGCAGGCTTCGAAGGAGATAGAACCATGGCTGATCCGGCGATTAAGCTC-3′ and 5′-GGGGACCACTTTGTACAAGAAAGCTGGGTCCTATGAGCTCTCATGGAAGTTTGC-3′). These constructs were introduced into *A. tumefaciens* strain GVG3101 pmp90. Four-week-old *N. benthamiana* plants were inoculated with the following combinations: YFN-CrDOF and YFC-CrDOF, YFN-CrDOF and YFC-CDF1, YFN-CrDOF and YFC-CDF2, and YFN-CDF2 and YFC-CDF2. As negative controls, pairs of YFC-CrDOF, YFC-CDF1, and YFC-CDF2 with YFN-AKIN10 were used. As positive controls, N- and C-terminal parts of AKIN10 were used, following the protocols described previously (Voinnet et al., 2003). Fluorescent interactions were visualized with a Leica TCS SP2/DMRE confocal microscope using an excitation wavelength of 514 nm.

CrDOF-Binding Assays

In order to assess if CrDOF was able to bind to *CrCO*, *CO*, and *FT* promoters, a similar transitory expression experiment in *N. benthamiana* leaves was used. In these experiments, 864 nucleotides from the *CrCO* promoter (5′-GGGGACAAGTTTGTACAAAAAAGCAGGCTTCACCATGGTGCAGGCATGCCGTGGCTCGGCAAG-3′ and 5′-GGGGACCACTTTGTACAAGAAAGCTGGGTCTCTCGCGTATAGAGGTGTGGT-3′), 1 kb from the *AtCO* promoter (5′-GGGGACAAGTTTGTACAAAAAAGCAGGCTTCACCATGGTAGTATAGAGTATCATCATAAACCC-3′ and 5′-GGGGACCACTTTGTACAAGAAAGCTGGGTCAATAACTCAGATGTAGTAAGTTTG-3′), and 1 kb from the *AtFT* promoter (5′-GGGGACAAGTTTGTACAAAAAAGCAGGCTTCACCATGGATTATATGTATAGATAGATTACCG-3′ and 5′-GGGGACCACTTTGTACAAGAAAGCTGGGTCCTTTGATCTTGAACAAACAGG-3′) were cloned first in pDONOR207 and then in pMDC110, which generates C-terminal fusions to *GFP* (p*CrCO*:*GFP*, p*CO*:*GFP*, and p*FT*:*GFP*). *N. benthamiana* leaves were inoculated with these constructs, while another set of *N. benthamiana* leaves were coinoculated with these constructs and 35S:*CrDOF*. GFP was visualized at 488-nm wavelength. Three independent inoculations were made for each studied condition. For each inoculation, three leaf fragments of the same size were analyzed (total of nine leaf fragments in three biological replicates), in which 11 or 12

randomly picked nuclei with positive signal were chosen, and GFP fluorescence was measured using MBF ImageJ. Therefore, signals from more than 100 nuclei were quantified per condition. Two versions of pCrCO, including 527 nucleotides (*pCrCO2*) and 285 nucleotides (*pCrCO3*), were constructed. Mutations at the binding sites were generated with the Muta-Direct Site-Directed Mutagenesis Kit from iNtRON Biotechnology following the instructions of the manufacturer.

C. reinhardtii Microscopy

CW15 and transgenic lines (*CrDOFox*:YFP) were observed using a confocal microscope (Leica TCS SP2/DMRE) for nuclear localization experiments. To visualize *C. reinhardtii* nuclei, SYTOBlue45 Fluorescent Nucleic Acid Stains (Molecular Probes) were used. Algae were grown in SD conditions in Sueoka medium supplemented with 10 mM NO_3^- until lag phase (3–4 μg mL^{-1} chlorophyll). One milliliter was collected by centrifugation (4 min, 5,500*g*) and suspended in 1 mL of Tris-buffered saline. One microliter of SYTOBlue45 and 1 and 5 μL of 10% (v/v) Triton X-100 for CW15 cells and transgenic lines, respectively, were added. After incubation for 10 min, cells were centrifuged and suspended in 100 μL of the same buffer. Finally, 3 μL of cells was mixed with 10 μL of 1.2% (w/v) low point fusion agarose at 30°C. The wavelengths used were 514 nm for YFP and 458 nm for SYTOBlue45.

Statistical Analysis

The statistical data presented in the figures and table are marked with asterisks and are means ± SE of three biological experiments or two biological experiments. The statistical significance between means of the different samples was calculated using a two-tailed Student's *t* test. Differences observed were considered statistically significant at $P < 0.05$ (*), $P < 0.01$ (**), and $P < 0.001$ (***).

Supplemental Data

The following supplemental materials are available.

Supplemental Figure S1. Protein characterization and phenotypic analysis of CrDOF.

Supplemental Figure S2. *CrDOF* functional analysis.

Supplemental Figure S3. CrDOF dimerization and DNA-binding activities.

Supplemental Figure S4. Effect of *CrDOF* expression in Arabidopsis.

Supplemental Table S1. *DOF* gene family in plants.

Supplemental Table S2. Presence of CrDOF protein complex in different conditions and lines.

Supplemental Table S3. Primers used in QPCR amplifications.

ACKNOWLEDGMENTS

We thank Fabio Fornara (University of Milan) for the *4cdf* mutant and Alicia Orea for help at the Instituto de Bioquímica Vegetal y Fotosíntesis microscopy/cytometry service.

Received March 2, 2015; accepted April 19, 2015; published April 20, 2015.

LITERATURE CITED

Amasino R (2010) Seasonal and developmental timing of flowering. Plant J **61:** 1001–1013

An H, Roussot C, Suárez-López P, Corbesier L, Vincent C, Piñeiro M, Hepworth S, Mouradov A, Justin S, Turnbull C, et al (2004) CONSTANS acts in the phloem to regulate a systemic signal that induces photoperiodic flowering of Arabidopsis. Development **131:** 3615–3626

Andrews S (2014) FastQC a quality-control tool for high-throughput sequence data. http://www.bioinformatics.babraham.ac.uk/projects/fastqc/ (January 2015)

Bailey TL, Boden M, Buske FA, Frith M, Grant CE, Clementi L, Ren J, Li WW, Noble WS (2009) MEME SUITE: tools for motif discovery and searching. Nucleic Acids Res **37:** W202–W208

Bisova K, Krylov DM, Umen JG (2005) Genome-wide annotation and expression profiling of cell cycle regulatory genes in *Chlamydomonas reinhardtii*. Plant Physiol **137:** 475–491

Bišová K, Zachleder V (2014) Cell-cycle regulation in green algae dividing by multiple fission. J Exp Bot **65:** 2585–2602

Bradford MM (1976) A rapid and sensitive method for the quantitation of microgram quantities of protein utilizing the principle of protein-dye binding. Anal Biochem **72:** 248–254

Camargo A, Llamas A, Schnell RA, Higuera JJ, González-Ballester D, Lefebvre PA, Fernández E, Galván A (2007) Nitrate signaling by the regulatory gene *NIT2* in *Chlamydomonas*. Plant Cell **19:** 3491–3503

Corbesier L, Vincent C, Jang S, Fornara F, Fan Q, Searle I, Giakountis A, Farrona S, Gissot L, Turnbull C, et al (2007) FT protein movement contributes to long-distance signaling in floral induction of Arabidopsis. Science **316:** 1030–1033

Davies DR, Plaskitt A (1971) Genetical and structural analyses of cell-wall formation in Chlamydomonas reinhardtii. Genet Res **17:** 33–43

Della Pina S, Souer E, Koes R (2014) Arguments in the evo-devo debate: say it with flowers! J Exp Bot **65:** 2231–2242

Edgar RC (2004) MUSCLE: multiple sequence alignment with high accuracy and high throughput. Nucleic Acids Res **32:** 1792–1797

Fornara F, Panigrahi KCS, Gissot L, Sauerbrunn N, Rühl M, Jarillo JA, Coupland G (2009) Arabidopsis DOF transcription factors act redundantly to reduce CONSTANS expression and are essential for a photoperiodic flowering response. Dev Cell **17:** 75–86

Goff L, Trapnell C, Kelley D (2013) cummeRbund: analysis, exploration, manipulation, and visualization of Cufflinks high-throughput sequencing data. R package version 2.10.0. http://www.bioconductor.org/ (January 2015)

Goodstein DM, Shu S, Howson R, Neupane R, Hayes RD, Fazo J, Mitros T, Dirks W, Hellsten U, Putnam N, et al (2012) Phytozome: a comparative platform for green plant genomics. Nucleic Acids Res **40:** D1178–D1186

Gualberti G, Papi M, Bellucci L, Ricci I, Bouchez D, Camilleri C, Costantino P, Vittorioso P (2002) Mutations in the Dof zinc finger genes *DAG2* and *DAG1* influence with opposite effects the germination of *Arabidopsis* seeds. Plant Cell **14:** 1253–1263

Harris EH (1989) The Chlamydomonas Source Book. Academic Press, San Diego

Hernando-Amado S, González-Calle V, Carbonero P, Barrero-Sicilia C (2012) The family of DOF transcription factors in Brachypodium distachyon: phylogenetic comparison with rice and barley DOFs and expression profiling. BMC Plant Biol **12:** 202

Ichihashi Y, Aguilar-Martínez JA, Farhi M, Chitwood DH, Kumar R, Millon LV, Peng J, Maloof JN, Sinha NR (2014) Evolutionary developmental transcriptomics reveals a gene network module regulating interspecific diversity in plant leaf shape. Proc Natl Acad Sci USA **111:** E2616–E2621

Imaizumi T, Schultz TF, Harmon FG, Ho LA, Kay SA (2005) FKF1 F-box protein mediates cyclic degradation of a repressor of CONSTANS in Arabidopsis. Science **309:** 293–297

Ito S, Song YH, Josephson-Day AR, Miller RJ, Breton G, Olmstead RG, Imaizumi T (2012) FLOWERING BHLH transcriptional activators control expression of the photoperiodic flowering regulator CONSTANS in Arabidopsis. Proc Natl Acad Sci USA **109:** 3582–3587

Jones DT, Taylor WR, Thornton JM (1992) The rapid generation of mutation data matrices from protein sequences. Comput Appl Biosci **8:** 275–282

Kloosterman B, Abelenda JA, Gomez MdelM, Oortwijn M, de Boer JM, Kowitwanich K, Horvath BM, van Eck HJ, Smaczniak C, Prat S, et al (2013) Naturally occurring allele diversity allows potato cultivation in northern latitudes. Nature **495:** 246–250

Kubista H, Edelbauer H, Boehm S (2004) Evidence for structural and functional diversity among SDS-resistant SNARE complexes in neuroendocrine cells. J Cell Sci **117:** 955–966

Lazaro A, Valverde F, Piñeiro M, Jarillo JA (2012) The *Arabidopsis* E3 ubiquitin ligase HOS1 negatively regulates CONSTANS abundance in the photoperiodic control of flowering. Plant Cell **24:** 982–999

Li D, Yang C, Li X, Gan Q, Zhao X, Zhu L (2009) Functional characterization of rice OsDof12. Planta **229:** 1159–1169

Lüders J, Pyrowolakis G, Jentsch S (2003) The ubiquitin-like protein HUB1 forms SDS-resistant complexes with cellular proteins in the absence of ATP. EMBO Rep **4:** 1169–1174

Matsuo T, Ishiura M (2010) New insights into the circadian clock in Chlamydomonas. Int Rev Cell Mol Biol **280:** 281–314

Merchant SS, Prochnik SE, Vallon O, Harris EH, Karpowicz SJ, Witman GB, Terry A, Salamov A, Fritz-Laylin LK, Maréchal-Drouard L, et al (2007) The Chlamydomonas genome reveals the evolution of key animal and plant functions. Science **318:** 245–250

Molnar A, Bassett A, Thuenemann E, Schwach F, Karkare S, Ossowski S, Weigel D, Baulcombe D (2009) Highly specific gene silencing by artificial microRNAs in the unicellular alga Chlamydomonas reinhardtii. Plant J **58:** 165–174

Moreno-Risueno MA, Martínez M, Vicente-Carbajosa J, Carbonero P (2007) The family of DOF transcription factors: from green unicellular algae to vascular plants. Mol Genet Genomics **277:** 379–390

Noguero M, Atif RM, Ochatt S, Thompson RD (2013) The role of the DNA-binding One Zinc Finger (DOF) transcription factor family in plants. Plant Sci **209:** 32–45

Papi M, Sabatini S, Bouchez D, Camilleri C, Costantino P, Vittorioso P (2000) Identification and disruption of an Arabidopsis zinc finger gene controlling seed germination. Genes Dev **14:** 28–33

Rensing SA, Lang D, Zimmer AD, Terry A, Salamov A, Shapiro H, Nishiyama T, Perroud PF, Lindquist EA, Kamisugi Y, et al (2008) The Physcomitrella genome reveals evolutionary insights into the conquest of land by plants. Science **319:** 64–69

Romero-Campero FJ, Lucas-Reina E, Said FE, Romero JM, Valverde F (2013) A contribution to the study of plant development evolution based on gene co-expression networks. Front Plant Sci **4:** 291

Ruijter JM, Ramakers C, Hoogaars WMH, Karlen Y, Bakker O, van den Hoff MJB, Moorman AF (2009) Amplification efficiency: linking baseline and bias in the analysis of quantitative PCR data. Nucleic Acids Res **37:** e45

Saitou N, Nei M (1987) The neighbor-joining method: a new method for reconstructing phylogenetic trees. Mol Biol Evol **4:** 406–425

Serrano G, Herrera-Palau R, Romero JM, Serrano A, Coupland G, Valverde F (2009) Chlamydomonas CONSTANS and the evolution of plant photoperiodic signaling. Curr Biol **19:** 359–368

Shigyo M, Tabei N, Yoneyama T, Yanagisawa S (2007) Evolutionary processes during the formation of the plant-specific Dof transcription factor family. Plant Cell Physiol **48:** 179–185

Shimogawara K, Fujiwara S, Grossman A, Usuda H (1998) High-efficiency transformation of Chlamydomonas reinhardtii by electroporation. Genetics **148:** 1821–1828

Sizova I, Fuhrmann M, Hegemann P (2001) A Streptomyces rimosus aphVIII gene coding for a new type phosphotransferase provides stable antibiotic resistance to Chlamydomonas reinhardtii. Gene **277:** 221–229

Skirycz A, Radziejwoski A, Busch W, Hannah MA, Czeszejko J, Kwaśniewski M, Zanor MI, Lohmann JU, De Veylder L, Witt I, et al (2008) The DOF transcription factor OBP1 is involved in cell cycle regulation in Arabidopsis thaliana. Plant J **56:** 779–792

Song YH, Smith RW, To BJ, Millar AJ, Imaizumi T (2012) FKF1 conveys timing information for CONSTANS stabilization in photoperiodic flowering. Science **336:** 1045–1049

Sueoka N, Chiang KS, Kates RJ (1967) Deoxyribonucleic acid replication in meiosis of Chlamydomonas reinhardtii. I. Isotopic transfer experiments with a strain producing eight zoospores. J Mol Biol **25:** 47–66

Tamaki S, Matsuo S, Wong HL, Yokoi S, Shimamoto K (2007) Hd3a protein is a mobile flowering signal in rice. Science **316:** 1033–1036

Tamura K, Peterson D, Peterson N, Stecher G, Nei M, Kumar S (2011) MEGA5: molecular evolutionary genetics analysis using maximum likelihood, evolutionary distance, and maximum parsimony methods. Mol Biol Evol **28:** 2731–2739

Trapnell C, Roberts A, Goff L, Pertea G, Kim D, Kelley DR, Pimentel H, Salzberg SL, Rinn JL, Pachter L (2012) Differential gene and transcript expression analysis of RNA-seq experiments with TopHat and Cufflinks. Nat Protoc **7:** 562–578

Umen JG, Goodenough UW (2001) Control of cell division by a retinoblastoma protein homolog in Chlamydomonas. Genes Dev **15:** 1652–1661

Valverde F (2011) CONSTANS and the evolutionary origin of photoperiodic timing of flowering. J Exp Bot **62:** 2453–2463

Varet A, Hause B, Hause G, Scheel D, Lee J (2003) The Arabidopsis *NHL3* gene encodes a plasma membrane protein and its overexpression correlates with increased resistance to *Pseudomonas syringae* pv. *tomato* DC3000. Plant Physiol **132:** 2023–2033

Vicente-Carbajosa J, Moose SP, Parsons RL, Schmidt RJ (1997) A maize zinc-finger protein binds the prolamin box in zein gene promoters and interacts with the basic leucine zipper transcriptional activator Opaque2. Proc Natl Acad Sci USA **94:** 7685–7690

Voinnet O, Rivas S, Mestre P, Baulcombe D (2003) An enhanced transient expression system in plants based on suppression of gene silencing by the p19 protein of tomato bushy stunt virus. Plant J **33:** 949–956

Yanagisawa S (1997) Dof DNA-binding domains of plant transcription factors contribute to multiple protein-protein interactions. Eur J Biochem **250:** 403–410

Yanagisawa S (2000) Dof1 and Dof2 transcription factors are associated with expression of multiple genes involved in carbon metabolism in maize. Plant J **21:** 281–288

Yanagisawa S, Schmidt RJ (1999) Diversity and similarity among recognition sequences of Dof transcription factors. Plant J **17:** 209–214

Supplemental Figure S1

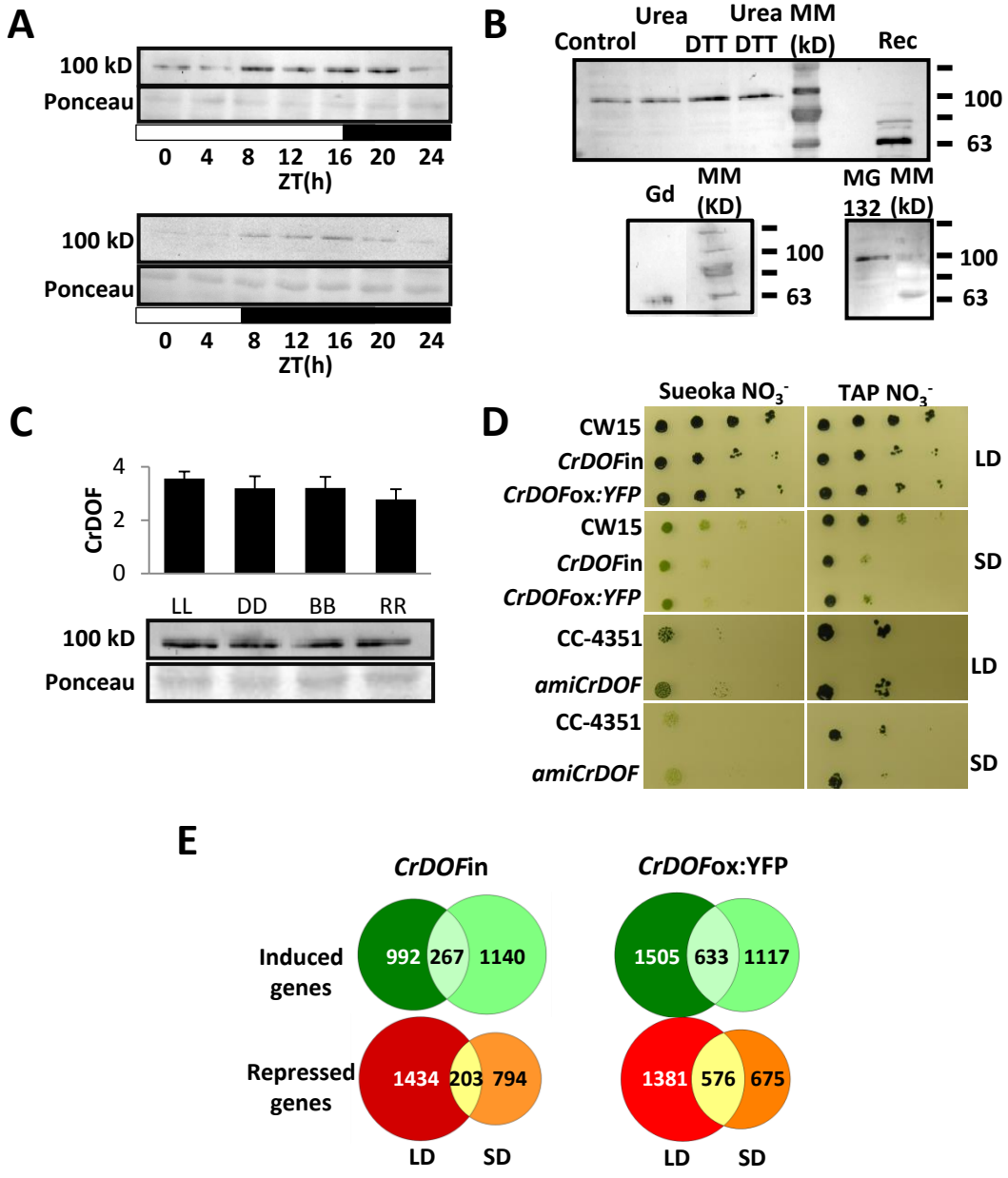

Supplemental Figure S2

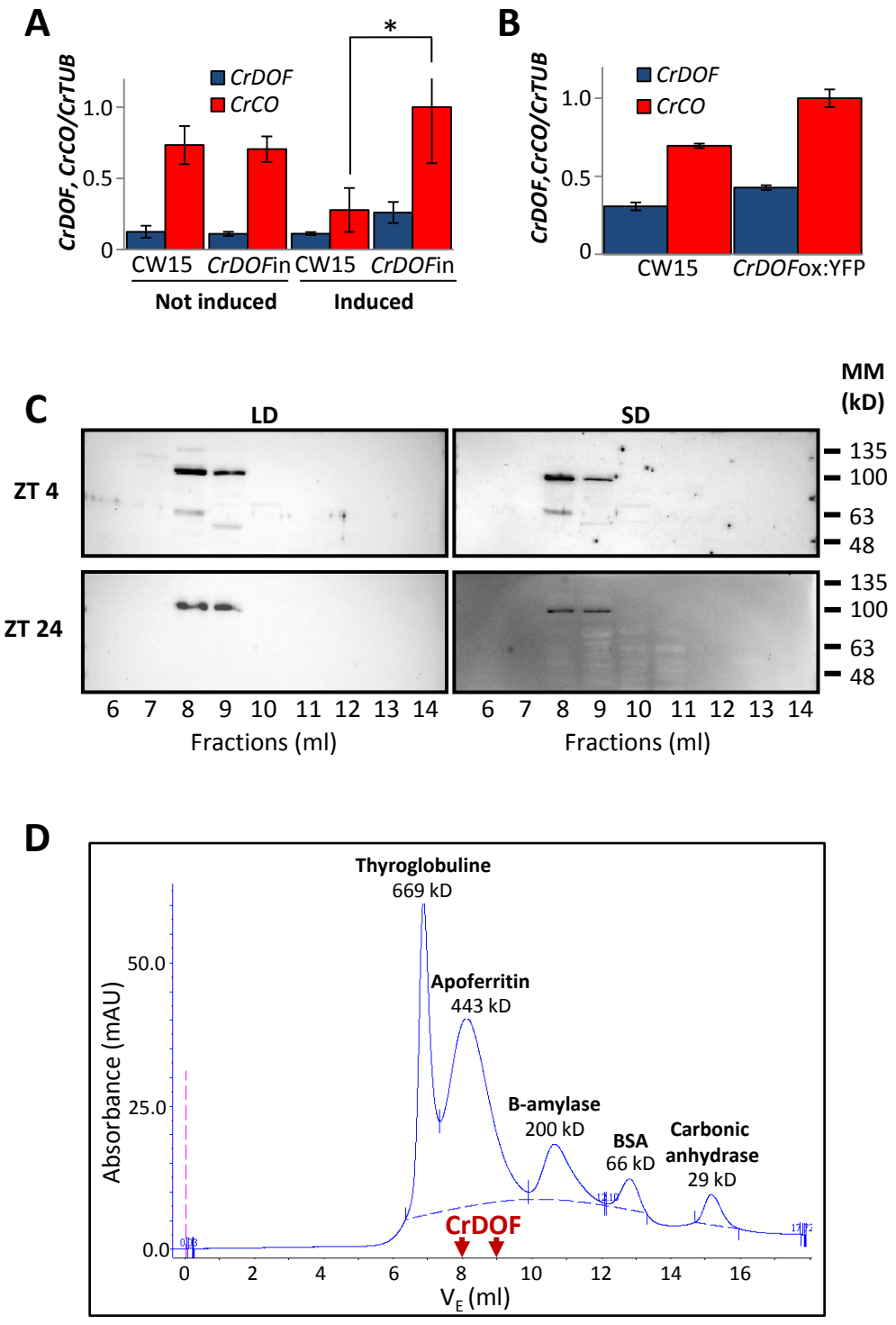

Supplemental Figure S3

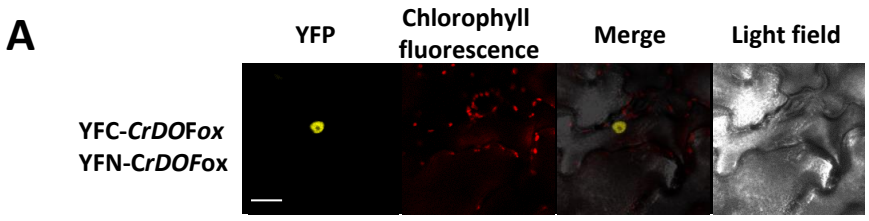

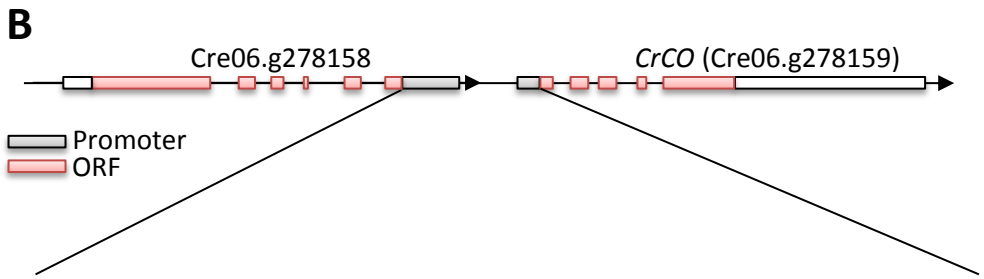

5`TGCAGGCATGCCGTGGCTCGGCAAGTCACGAGACAGAGCATGCTTTATCAAGGTAGGCAGCT
GCAGCGGCTCGGACTGATTTGAAGTGGGGGTGGCACGTGGAGGGATCGACGGGCCCTGCTGA
GGTTGCGGTGGAGGTCACTAGCAACTGCGCTCAGCTAGCGCATGGCTGTAGAGGCTCGCGACA
ATAAAGCGTGCCGGCTGTCCTTTCTGGAAGCTGGGCGGCCAAGCTTGCTAAGGACTTCCAAGCG
GGGTGAGAAGGGACAAGCAGGGGCACTCCAGCTGTGAGCAGGCCCTGAGTAGGACGGACGTG
GCTGGAGCCGTGGAACCGTTAAGCTGGGAATGAGGTTTTTAGGTGACAGCAGTGTACGTGCGG
ATAGCTGCATTTGCGCGTTGCTCGGATGGCGTGGATATGTGTTGCAGCAAGGATAAAGGTTTCC
GGCACGGGCGTTACGTATACCGTTGTCGAAGGCGGCCTAACTTCGCTGCCGCCGTGAAACGTCG
CTTCTTGTAAGCTACGCCCATGTATCGGCAGATTGCGCTGCGTGCATCGGATCGGGCCGAGTTAT
AGACGAATCTGAAACGCCGACATGTTCGCGAACTGGCTCCACAGCGTACTTTGTTGAGTTTTGT
TGCACGTACCACTGACATTGCGATAACATATAAGGCTAGAGATCAAGTTAAAGCAGGGGCGCG
AGTCGGCCGACGGCCCCGTTGCATGGGGTGCTTGCTGGACGGTGAAGACGAGAGCTCTCGCCT
CAAAGGTTCAGTCCCCAACGCTTGCACATTTGCCCTAAACGCAATACTCCCCAACAACACAAAT
ATACCACACCTCTATACGCGAGAATGTCGAGTTGCGTCGTGTGCGCGGCCGCAGCGGTCGTTTG
GTGCCAGAATGACAAGGCGCTGCTTTGCAAGGACTGCGATGTGCGCATCCACACCAGCAACGC
GGT **3`**

Binding site mutations:

1. GGCTCCACAGCGTA**CaaT**GTTGAGTTTTGTTGC (p*CrCO*3:GFP*).
2. CTAGAGATCAAGTT**AttG**CAGGGGCGCGAG (p*CrCO*3:GFP**).
3. GAGCTCTCGCCTC**AttG**GTTCAGTCCCCA (p*CrCO*3:GFP***).

Supplemental Figure S4

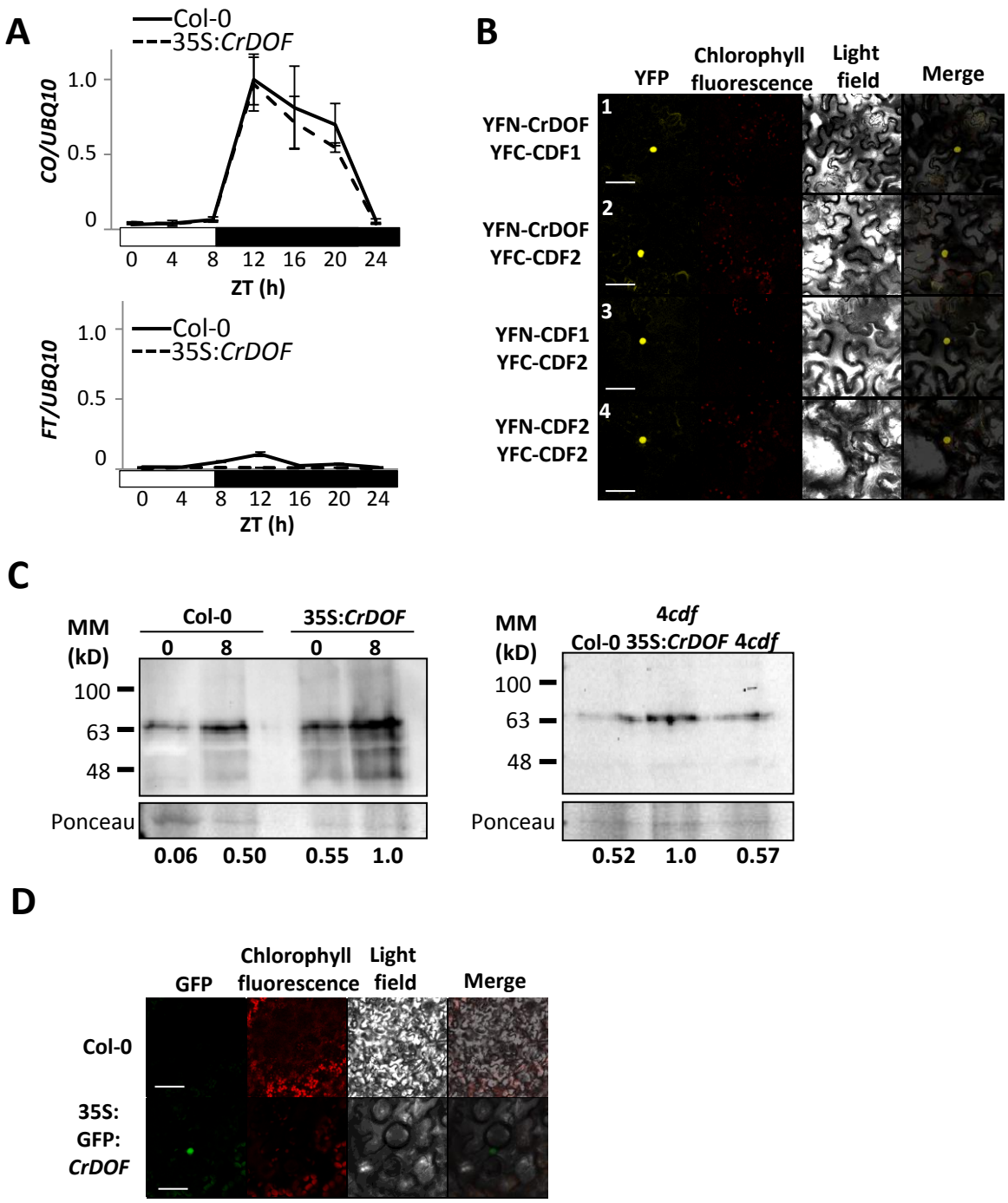

Supplemental Table S1. ***DOF*** gene family in plants.

	Gene Name	Accession number
A. thaliana	AtCOG1	At1g29160
	AtDAG1	At3g61850
	AtDAG2	At2g46590
	AtDOF1.3	At1g26790
	AtDOF1.8	At1g64620
	AtDOF3.2	At3g45610
	AtDOF4.1	At4g00940
	AtDOF4.6	At4g24060
	AtDOF5.6	At5g62940
	AtOBP3	At3g55370
	AtTMO6	At5g60200
	CDF1	At5g62430
	CDF2	At5g39660
	CDF3	At3g47500
	CDF4	At2g34140
	CDF5	At1g69570
C. reinhardtii	CrDOF	Cre12.g521150
M. pusilla	MpDOF	MpEEH5513
O.sativa	OsDOF2	Os01g15900
	OsDOF4	Os01g17000
	OsDOF9	Os02g45200
	OsDOF12	Os03g07360
	OsDOF14	Os03g16850
	OsDOF16	Os03g60630
	OsDOF18	Os04g47990
	OsDOF21	Os07g13260
	OsDOF23	Os07g48570
	OsDOF26	Os10g26620
O. tauri	OtDOF	Ot04g03010
P. patens	PpDOF1	Pp1s69_113V6
	PpDOF2	Pp1s341_43V6
	PpDOF3	Pp1s170_42V6
	PpDOF4	Pp1s124_139V6
	PpDOF5	Pp1s26_282V6
	PpDOF6	Pp1s149_180V6
	PpDOF7	Pp1s68_214V6
	PpDOF8	Pp1s169_171V6
	PpDOF9	Pp1s177_76V6
	PpDOF10	Pp1s1_286V6
	PpDOF11	Pp1s118_226V6
	PpDOF12	Pp1s12_364V6
	PpDOF13	Pp1s199_87V6
	PpDOF14	Pp1s351_46V6
	PpDOF15	Pp1s385_53V6
	PpDOF16	Pp1s392_2V6

	Gene Name	Accession number
P. tricocharpa	PtDOF5	POPTR_0010s21240
	PtDOF6	POPTR_0017s12080
	PtDOF8	POPTR_0009s03490
	PtDOF13	POPTR_0004s12120
	PtDOF14	POPTR_0004s05580
	PtDOF15	POPTR_0004s04590
	PtDOF16	POPTR_0013s06290
	PtDOF17	POPTR_0003s02890
	PtDOF18	POPTR_0003s14450
	PtDOF20	POPTR_0011s07400
	PtDOF21	POPTR_0011s05410
	PtDOF27	POPTR_0007s11790
	PtDOF32	POPTR_0015s01160
	PtDOF33	POPTR_0015s08810
	PtDOF37	POPTR_0002s17490
	PtDOF38	POPTR_0019s05720
	PtDOF42	POPTR_0005s13990
	PtDOF44	POPTR_0014s09640
	PtDOF48	POPTR_0014s03590
	PtDOF51	POPTR_0008s08740
	PtDOF52	POPTR_0001s24540
	PtDOF57	POPTR_0001s11130
	PtDOF59	POPTR_0012s08280
	PtDOF60	POPTR_0012s02570
	PtDOF61	POPTR_0012s12670
V. carteri	VcDOF	Vc20003744
Z. mays	ZmDOF3	GRMZM2G146283
	ZmDOF8	GRMZM2G463525
	ZmDOF9	AC155434.2_FG006
	ZmDOF17	GRMZM2G114998
	ZmDOF21	GRMZM2G162749
	ZmDOF23	GRMZM2G010290
	ZmDOF27	GRMZM2G017470
	ZmDOF28	GRMZM2G093725
	ZmDOF29	GRMZM2G140694
	ZmDOF36	GRMZM2G137502
	ZmDOF40	GRMZM2G138455
	ZmDOF43	GRMZM2G589696
	ZmDOF44	AC233935.1_FG005

The name and accession numbers of *DOF* genes from *Arabidopsis thaliana, Chlamydomonas reinhardtii, Micromonas pusilla, Oriza sativa, Ostreococcus tauri, Physcomitrella patens, Populus tricocharpa, Volvox carteri* and *Zea mays* used in the phylogenetic studies of this work are shown.

Supplemental Table S2. Presence of CrDOF protein complex in different conditions and lines.

		Long Day				Short Day			
		ZT 4		ZT 24		ZT 4		ZT 24	
		Complex Size (kD)		Complex Size (kD)		Complex Size (kD)		Complex Size (kD)	
	MM (kD)	464 kD	314 kD	464 kD	314 kD	464 kD	314 kD	464 kD	314 kD
CW15	100 kD	49.5	19.2	32.2	38.7	41.7	10.8	7.1	6.7
	62 kD	4.8				7.6			
*CrDOF*in	100 kD	—	—	42.7	24.1	—	—	31.2	2.5
	62 kD	—	—	6.2	0.6	—	—	3.4	0.9

The presence and absence of the complex including CrDOF in two consecutive fractions (#8 and #9) of the gel-filtration column (Supplemental Fig. 2C-D) are shown. Both CW15 and *CrDOF*in lines in LD and SD conditions were analysed and the molecular mass (MM) in kD, annotated. The presence of the 100 kD and 60 kD bands is shown including an estimated quantitation: Maximum (red), medium (orange and yellow) and minimum (pale yellow) amount of protein. Not detected protein (white); not analysed (-).

Supplemental Table S3. Primers used in QPCR amplifications.

***Chlamydomonas* Genes**	**Sequence**	**Size (bp)**
CrDOF	5'- GTCGTCTGGCAGCTACGC -3' 5'- CACCTAGCACCCGAGTAAGC -3'	70
CrCO	5'- CTTCCCGCAAGGCGTATGC -3' 5'- GCCTCAATCTCCTCCTTCTTGGC -3'	73
CrCYCA1	5'- CGGCATTCACCGCTCGTGAG -3' 5'- AGCGTCATGTACGATAGCGTGG -3'	145
CrCDKB1	5'- GGATAAGGTGACCGTGGACGC -3' 5'- AGACTTCGCACCCTTGCACG -3'	149
CrTUB	5'- GTTGCATCGTTAGCGTGGACG -3' 5'- GCAGCAGCCAATGTTCAGACT -3'	170
Arabidopsis Genes	**Sequence**	**Size (bp)**
CO	5'- CCAATGGACAGAGAAGCCAGG -3 5'- GCATCGTGTTGAACCCTTGC -3'	70
FT	5'- CGAACGGTGATGATGCCTATAGTAG -3' 5'- CACTCTCATTTTCCTCCCCCTCTC -3'	73
UBQ10	5' -GAAGTTCAATGTTTCGTTTCATGT-3' 5' - GGATTATACAAGGCCCCAAAA -3'	145